Modeling and Verification of Advanced Under-Frequency Load Shedding Schemes

Master of Science Thesis

Meng Zhang

TU Delft Delft University of Technology

Challenge the Future

Modeling and Verification of Advanced Under-Frequency Load Shedding Schemes

Master of Science Thesis

by

Meng Zhang

in partial fulfillment of the requirements for the degree of
Master of Science

in Electrical Sustainable Energy

Department of Intelligent Electrical Power Grids (IEPG)

Faculty of Electrical Engineering, Mathematics, and Computer Science (EEMCS)

Delft University of Technology

To be defended publicly on 21st November 2016 at 11:00 AM

Supervisors:	Prof. Mart van der Meijden Dr. Marjan Popov MSc. Ilya Tyuryukanov
Thesis Committee:	Prof. Mart van der Meijden Dr. Marjan Popov Dr. Mohamad Ghaffarian Niasar

Acknowledgement

First of all, I would like to express my gratitude to my supervisor Ilya Tyuryukanov who has consistently helped me with the thesis project. His constant academic guidance as well as personal support have been truly helpful and inspirational for the development of my work.

I would like to thank Dr. Marjan Popov for providing the opportunity to me to do the research that has greatly raised my interest in the field of power system. The master courses he teaches such as Power System Analysis and Power System Grounding and Protection are very helpful for my professional knowledge and skills.

A special thanks goes to my friends, Aimilia, Digvijay, Chetan, Nishant, Shuang, Adedotun and many others. Thank you for providing all the moral and mental support to me and many valuable discussions that have considerably expanded my understanding of power systems. Being friends with you has been the greatest experience in my life and I would like to give you my sincere appreciation.

I would also like to take this opportunity to thank Ellen, our department secretary, for helping me with all the routine things and arrangements.

My thanks to my parents are always beyond word. During the two-year study, they have provided me incredible encouragement and support.

Meng Zhang

Delft, November 2016

Abstract

Power system blackouts have been observed increasingly frequent and severe. As an emergency control action to rescue the system from complete blackout, under-frequency load shedding (UFLS) technique can disconnect a part of the load when a disturbance occurs and an excessively low frequency is detected.

Traditional UFLS scheme is widely adopted in present power systems. However, it usually has several pre-defined steps and corresponding frequency thresholds without sufficient consideration of the actual system characteristics and the disturbance situations. This can result in inaccurate load shedding or even unsuccessful protection.

In comparison, advanced UFLS schemes proposed in the literature can dynamically adjust the shedding steps based on the specified algorithms and thus are advantageous over traditional UFLS scheme in frequency recovery and other aspects such as reducing total shedding amount and improving voltage stability.

In the thesis, a set of models are developed using PowerFactory and Python for advanced UFLS schemes. Then three schemes are implemented and verified. Simulation results show that these schemes can successfully arrest frequency decline along with specified optimizations. Several factors such as load characteristics are observed to have significant impact on the UFLS performance. For one of the considered schemes, a step correction method is proposed in the thesis to improve the frequency performance for more disturbance scenarios.

Key words: Under-Frequency Load Shedding, Power Imbalance Estimation, PowerFactory, Python

Table of Contents

List of Figures

List of Tables

List of Symbols

Name	Unit	Description
H	s	Inertia constant
ω	rad/s	Rotational speed
ω_s	rad/s	Synchronous rotational speed
P_{L0}	MW	Total pre-fault load active power in the island
P_{def}	p.u.	Active power deficiency as percentage of P_{L0}
P_{L0i}	p.u.	Pre-fault active power of ith load
Q_{L0i}	p.u.	Pre-fault reactive power of ith load
P_{Li}	p.u.	Active and reactive power of ith load
Q_{Li}	p.u.	Reactive power of ith load [p.u.]
V_{Li}	p.u.	Voltage of ith load [p.u.]
V_{L0i}	p.u.	Pre-fault voltage of ith load [p.u.]
ΔV_i	p.u.	Voltage deviation of ith load immediately after the disturbance
α_i	1	Voltage dependency on active power of ith load
β_i	1	Voltage dependency on reactive power of ith load
S_{sys}	MVA	Equivalent apparent power of the system
H_{sys}	s	Equivalent inertia constant of the system
f_n	Hz	Nominal frequency (60 in the IEEE 39 bus test system)
f	Hz	Electrical frequency
f_{COI}	Hz	Center of inertial frequency of the island
N_L	1	Number of loads in the island
N_G	1	Number of generators in the island
$P_{shed,i}$	1	Shedding amount of ith load as a fraction of P_{L0}
P_{shed}	1	Total shedding amount as a fraction of P_{L0}
K_i	1	Distribution factor of ith load
Δf_{Li}	Hz	Frequency deviation of ith load immediately after the disturbance
VQS_i	1	Voltage sensitivity on reactive power of ith load
$P_{tracing,i}$	MW	Contribution of active power from lost generators to ith load
$f_{th,i}$	Hz	Frequency threshold of the first load shedding step
$P_{step,i}$	1	Initial shedding amount of the ith step as a fraction of P_{def}
$P'_{step,i}$	1	Adjusted shedding amount of the ith step as a fraction of P_{def}
$ROCOF_{min}$	Hz/s	Recorded minimum ROCOF value in the time window
Δ_i	1	ROCOF change before the ith step as a fraction of $ROCOF_{min}$
T_{delay}	s	Time delay
$P_{flow,ij}$	MW	Active power flow from bus i to bus j
$P_{Gj,Li}$	MW	Active power contributed by generators at bus j to the load at bus i
$P_{loss,ij}$	MW	Active power loss of the line connecting bus i and bus j
P_{Gi}	MW	Active power generated at bus i

List of Acronyms

UFLS	Under Frequency Load Shedding
WAM	Wide Area Measurement
SCADA	Supervisory Control and Data Acquisition
ROCOF	Rate of Change of Frequency
COI	Center of Inertia
VQS	Voltage Reactive Power Sensitivity
DSL	DIgSILENT Simulation Language

1 Introduction

Chapter Summary: This chapter introduces the background of the thesis. Then the motivation of the study on advanced under-frequency load shedding is justified. Finally, the thesis objective and structure are provided.

1.1 Power System Blackouts

Over the past few decades, electric power systems around the globe have seen massive changes such as rapid growth of installed capacities, restructuring and deregulation of the electrical industry, and extensive integration of renewable energy sources. These changes have been accompanied with more frequent and severe occurrence of cascading failures and blackouts.

The North America blackout that happened on 14 August 2003 was one of the worst cascading failures in the history of power system around the world [1]. The cascading failure can be traced back to the morning of that day when there was a reactive power supply issue, which unfortunately did not raise sufficient early awareness due to software problems. The event gradually unfolded when several tree contacts consecutively occurred and one generator tripped due to overexcitation. Until this moment, the blackout could have been prevented by under frequency load shedding or system readjusting [2]. But when the Sammis-Star 345kV line tripped due to a zone 3 relay action, the widespread cascading reached a no-return point, hundreds of other lines tripped, and 5 minutes later the whole north-east system collapsed.

In the same year two other major blackouts happened on the European continent. One of them that occurred on 23 September in the Nordic system began with several system components out of service for scheduled maintenance. The critical event was a nuclear plant outage due to a valve problem and an ensuing double bus bar fault 5 minutes later. This directly led to a collapse of both frequency and voltage. Consequently, a region of southern Sweden and eastern Denmark was separated and collapsed to blackout in a matter of seconds.

The other blackout happened in Italy on 28 September 2003 and resulted in the entire Italian power system collapsed. The cascading outage began with a heavy power import from Switzerland to Italy. When two transmission lines were tripped within seconds because of a tree contact, the heavy power flow was shifted to the adjacent lines that connected Italy and France, Austria, and Slovenia. As a result, all major tie lines of Italy were tripped in minutes, leading to a nation-wide loss of power.

The exact mechanics of power system blackouts is complex and varies dramatically in different situations. But many blackouts observed in the literature such as [3] and [4] progressed in a common patter as shown in Figure 1-1.

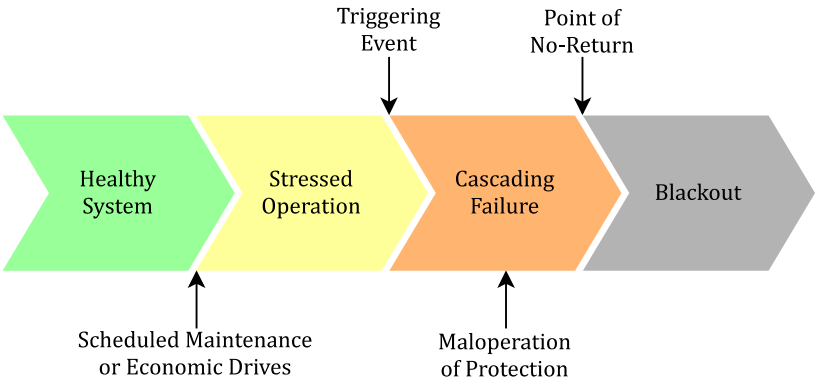

Figure 1-1: A Generalized Blackout Pattern

It can be roughly generalized that most of cascading failures started with a stressed operation [5] due to scheduled maintenance or peak hour situation that may cause the system safety margin to be narrowed. Once a triggering event occurs, such as a natural disaster or an unscheduled outage of components, an overload situation may arise in the area. Accompanied by maloperation of protection schemes that are in duty, the situation can escalate rapidly and lead to a cascading tripping of elements. Before the cascading failure reaches the point of no return, which is elaborated in reference [6], fast and appropriate protection schemes are still able to rescue the system before the collapse. But complete blackout becomes unavoidable once major generation units and tie lines are tripped due to excessive under-frequency and under-voltage.

1.2 Under-Frequency Operation

Equation (1-1) is the swing equation that describes the mechanical motion of a generator.

$$\frac{2H}{\omega_s}\frac{d\omega}{dt} = P_m - P_e \tag{1-1}$$

where H is Inertia constant [s]
ω_s is Synchronous rotational speed [rad/s]
ω is Rotational speed [rad/s]
P_m is Input mechanical power [p.u.]
P_e is Output electrical power [p.u.]

Power systems and all its components are designed to run at nominal frequency. From equation (1-1), it can be easily noticed that when the system operates with a shortage of generation (mechanical) power as compared to load (electrical) power, the electrical frequency will decrease. Although most devices can withstand a small frequency deviation, the magnitude and duration of the deviation is strictly limited especially for costly units such as synchronous generators. Generator turbines are vulnerable to abnormal frequency operation due to excessive vibration that can result in blade fatigue and acceleration of aging. According to [7], a steam turbine can persist no more than 100 minutes when there is a 2% change of rotational frequency from the nominal value, as shown in Table 1-1.

Table 1-1: Operation Capability of an Example Steam Turbine

Frequency Deviation at Full Load	Maximum Operating Time
$\Delta f = 1\% f_n$	Continuously
$\Delta f = 2\% f_n$	100 minutes
$\Delta f = 3\% f_n$	10 minutes
$\Delta f = 4\% f_n$	1 minute
$\Delta f = 5\% f_n$	0.1 minutes
$\Delta f = 6\% f_n$	1 second

In addition, power plant auxiliary devices such as induction machines in the cooling system heavily rely on a stable frequency. Lower frequency results in less rotational speed and less effective ventilation.

1.3 Conventional UFLS and the Limitations

Currently there are several known solutions to mitigate cascading outages and rescue the power system before the complete blackout. These solutions include out-of-step tripping and blocking, line switching, generator rescheduling, controlled system separation, load shedding, etc. Among them under-frequency load shedding (UFLS) has been widely adopted in power systems as an emergency action for arresting the frequency decline and thus preventing cascading failure due to abnormal network conditions. The principle of UFLS is to intentionally curtail a part of power system load when an excessively low electrical frequency is detected in order to mitigate or eliminate the power imbalance and thus to help frequency recovery.

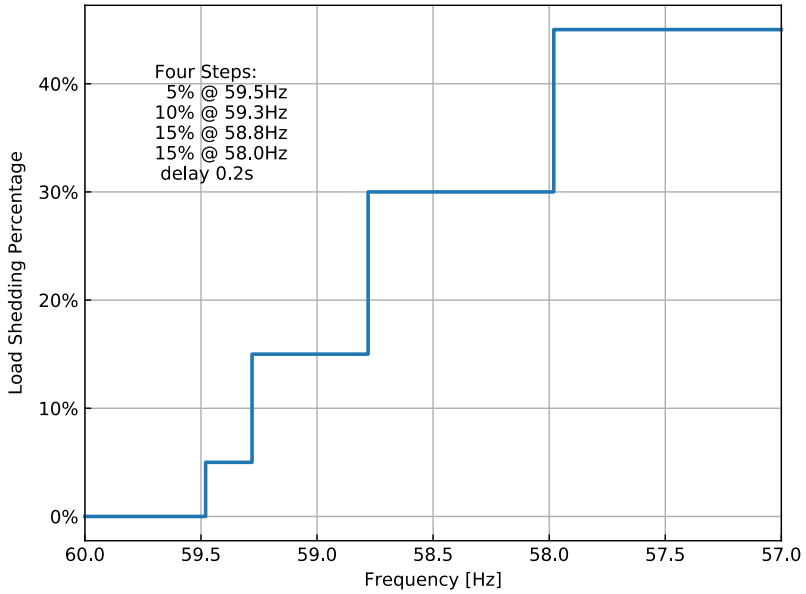

Figure 1-2: A Four-Step Conventional UFLS Scheme

Conventionally, UFLS involves several pre-defined load shedding steps, each of which is associated with a frequency threshold. Once the measured frequency reaches one of the thresholds, the corresponding under-frequency relay will be given the order to disconnect a certain percentage of load on a bus. Figure 1-2 from reference [8] shows a typical 4-step load shedding scheme.

Although the conventional UFLS scheme is widely implemented in existing power systems [9], it has the following several main drawbacks that can result in malfunction and inability to prevent the cascading failure, examples of which can be found in [10].

1. Conventional UFLS ignores dynamic behavior of power system loads. During the cascading outage, frequency decline is accompanied by voltage decrease, which in turn decreases the active power consumption of voltage dependent loads. In this way, the load dependency on voltage seems to have alleviated the over-load situation, but the actual generation deficiency is larger than what appears to be. Even if UFLS has curtailed a part of the load, voltage instability issues remain unresolved.
2. Conventional UFLS ignores the disturbance location in the load shedding decision process. According to the observation of reference [11], frequency falls faster in the adjacency of disturbance than in the undisturbed area. But the conventional UFLS sheds the same fraction of load at each bus at the same time, which may lead to unwanted redistribution of power flow and excessive increasing of the loading on major tie lines.
3. Fixed steps of the conventional UFLS cannot dynamically adapt itself to the power imbalance, thus unable to proceed an accurate load shedding. This can lead to over-shed or under-shed which may cause an unsatisfactory frequency excursion after the load shedding process.

1.4 Thesis Objective and Structure

Due to the deficiencies of conventional UFLS schemes, many advanced UFLS schemes have been developed to improve the protection effectiveness. In the literature, proposed schemes use various external signals and algorithms to change the load shedding pattern in a dynamic way to not only arrest frequency decline, but also enhance other aspects such as reduction of the shedding amount and improvement in voltage stability margin. In addition, recent development of the Supervisory Control and Data Acquisition (SCADA) system and the Wide Area Measurement (WAM) system has made immediate access to the power system state easy and fast calculation available.

Based on the above-mentioned facts, the objective of the thesis is to develop a set of models using PowerFactory and Python for several selected advanced UFLS schemes. The performance and limitations of the schemes will then be verified with respect to various disturbance scenarios using the developed models in the IEEE 39-bus test system.

The thesis consists of six chapters. Chapter 2 is a literature review on the development of UFLS schemes and a brief description of their principles. Chapter 3 introduces the methodology in the implementation of the schemes including software environment, general process and basic assumptions. Chapter 4 implements and investigates one selected advanced UFLS scheme with adaptive steps. To improve the performance of this scheme, a correction method is proposed in this chapter. Simulation results show that the proposed correction method can effectively find a balance point between satisfying the IEEE objectives and reducing the total shedding amount in various disturbance scenarios and load conditions. Chapter 5 is concerned with two other advanced UFLS schemes which use the power flow tracing method and the voltage-reactive power sensitivity method respectively to distribute the load shedding amount. In this chapter, simulations are also conducted which showed that the power flow tracing method is better than the voltage-reactive power sensitivity method in terms of voltage stability and computational effort. Chapter 6 gives the conclusions of this thesis research and an outlook into future works to continue the present development.

2 Literature Review

Chapter Summary: This chapter consists of a literature review on the development of UFLS schemes. Section 2.1 introduces the development of the conventional UFLS schemes. Section 2.2 focuses on the state-of-the-art schemes and various algorithms involved in optimization of protection processes.

2.1 Development of Conventional UFLS Schemes

In 1950 the UFLS problem was reviewed by the Operating Committee of the Northwest Power Pool [12]. At that time, some basic principles, as well as generally allowed frequency swing ranges and regular protection methods, of solving the UFLS problem were suggested. Later in reference [13] the rate of change of frequency (ROCOF) was proposed to be related to the severity of the disturbance and relays that can act on ROCOF are suggested to be implemented along with under-frequency relay.

The prototype of UFLS in the USA as disconnecting in steps was not readily developed until 1971 when a guideline was proposed in the East Central Area Reliability Agreement [14]. In this guideline, it specifically indicates what percentage of load should be shed and at which level of frequency should the load shedding actions take place.

Benefiting from the modernization of electrical power systems as well as other knowledge fields, UFLS schemes have been under constant development to improve system stability and frequency performance. Reference [8] proposed an improved load shedding program based on the load power reduction due to frequency reduction, namely load dependency on frequency. It is suggested in that paper that the number of shedding steps between 3 and 5 will provide the best shedding accuracy. In reference [15] it is concluded that the initial steps of the load shedding program should be adjusted to a larger size compared to the last few steps to improve the frequency recovery process. Reference [16] also strengthens the idea of increasing the amount of the first three steps, in addition to an improved coordination with the spinning reserve to achieve a better frequency excursion.

Many other authors ([17]-[22]) have proposed their own improved versions of the traditional UFLS, all verified in their specific test systems. These schemes use various technologies such as fuzzy logic and gradient projection and should be well acknowledged. However, these schemes operate independently from the disturbance neglecting the disturbance magnitude and the load characteristics. The fixed load shedding steps are not able to adapt itself in accordance with the actual over-load situation and system characteristics, and thus should be further improved.

2.2 Development of Advanced UFLS Schemes

Distinct from traditional UFLS, the advanced schemes investigated in the thesis can estimate the generation deficiency immediately after the disturbance and accordingly change the shedding schedule in order to achieve an acceptable frequency recovery as well as other optimization aspects. Due to the recent development of the Supervisory Control and Data Acquisition (SCADA) system and the Wide Area Measurement (WAM) system, more power system state information becomes instantly accessible, making the connection between the estimation of disturbances and load shedding process possible.

2.2.1 **Power Deficiency Estimation**

As a common characteristic of the considered advanced ULFS schemes, power deficiency estimation is based on the aggregated frequency response model that was proposed in [23]. In that paper, the authors proposed a simplification method which significantly reduced the complexity of frequency response model of a synchronous generator. The method considered only the midrange frequencies, and neglected some components of the generator model including the boiler thermal system and the generator frequency response. The active power deficiency of a generator that causes the initial decrease of frequency can be expressed as [23].

$$\Delta P = \frac{2H}{\omega_s}\frac{d\omega}{dt}\bigg|_{t=0} \tag{2-1}$$

where ΔP is Active power deficiency of a generator [p.u.]
ω is Rotational speed [rad/s]
ω_s is Synchronous rotational speed [rad/s]

An improved algorithm was proposed [24] for the estimation which considered the load active power dependency on voltage as a parameter. The power consumed by the loads is generally not constant and may be changed dynamically with the voltage and frequency. A commonly adopted method to model the relationship between the load voltage and the consumed power is to use an exponential equation, as shown below in equation (2-2) and (2-3) [25].

$$P_{Li} = P_{L0i}\left(\frac{V_{Li}}{V_{L0i}}\right)^{\alpha_i} \tag{2-2}$$

$$Q_{Li} = Q_{L0i}\left(\frac{V_{Li}}{V_{L0i}}\right)^{\beta_i} \tag{2-3}$$

where P_{L0i} is Pre-fault active power of ith load [p.u.]
Q_{L0i} is Pre-fault reactive power of ith load [p.u.]
P_{Li} is Active and reactive power of ith load [p.u.]
Q_{Li} is Reactive power of ith load [p.u.]
V_{Li} is Voltage of ith load [p.u.]
V_{L0i} is Pre-fault voltage of ith load [p.u.]
α_i is Voltage dependency on active power of ith load
β_i is Voltage dependency on reactive power of ith load

For composite system loads, the exponent α usually ranges between 0.5 and 1.8, and the exponent β is typically between 1.5 and 6 [25]. In special cases, when α is equal to 0, 1 and 2, the model is regarded as being of constant power, constant current, and constant impedance, respectively. Reference [26] estimated the exponent values α and β of various loads based on the measured voltage and current, as shown in Table 2-1.

Table 2-1: Estimated Values for Power Dependency Factors of Different Types of Loads

Load	$\boldsymbol{\alpha}$	$\boldsymbol{\beta}$
Radiator	1.96	-
LED bulb	0.83	0.92
Fan	2.66	3.60
Idling induction motor	4.05	3.29
Induction motor with frequency converter	2.61	2.53

Through a series of calculation, the improved power deficiency estimation for a multi-machine system is expressed as equation (2-4) [24]. Here the power deficiency is assumed to be a fraction of the total pre-fault load power for convenience.

$$P_{def} = \frac{2H_{sys}S_{sys}}{P_{L0}f_n}\frac{df_{COI}}{dt} + \frac{1}{P_{L0}}\sum_{i=1}^{N_L} P_{L0i}\left[\left(\frac{V_{Li}}{V_{L0i}}\right)^{\alpha_i} - 1\right] \tag{2-4}$$

$$S_{sys} = \sum_{j=1}^{N_G} S_j \tag{2-5}$$

$$H_{sys} = \frac{1}{S_{sys}}\sum_{j=1}^{N_G} H_j S_j \tag{2-6}$$

where S_{sys} is Equivalent apparent power of the system [MVA]
H_{sys} is Equivalent apparent inertia constant of the system [s]
S_j is the rated apparent power of jth machine
H_j is the inertia constant of jth machine based on its own rated apparent power
P_{L0} is Total pre-fault load power in the island [MW]
P_{def} is Generation power deficiency (fraction of P_{L0})
f_n is Nominal frequency [Hz]
f_{COI} is Center of Inertia electrical frequency [Hz]
N_L is Number of loads in the system
N_G is Number of generators in the system

This estimation method is adopted in the present thesis as the basis for implementing the advanced UFLS schemes. Simulations showed that the estimation has an acceptable accuracy in various disturbance scenarios and load conditions. The results will be displayed in section 3.2.3.

With the help of the improved estimation of power deficiency, modern UFLS schemes proposed in the literature are theoretically capable of optimizing frequency recovery and maintaining system stability. This capability is achieved in two ways. First, the initial total shedding amount is assigned as the estimated power deficiency instead of a pre-defined fixed value to achieve a more accurate UFLS process. Second, the actual shedding amount is dynamically adjusted according to certain external signals so that other considerations such as the minimization of the load shedding amount or voltage stability can be included during the load shedding process.

In order to dynamically adjust the load shedding steps, the advanced UFLS schemes in general are designed in two directions, which are named in this thesis as step-oriented adaptation and topology-oriented adaptation, respectively. The step-oriented adaptation is to alter each step according to external signals such as rate of change of frequency (ROCOF). These schemes usually assume that every under-frequency relay in the affected area will disconnect the same percentage of the associated load on a bus. The topology-oriented adaptation is to distribute the total shedding amount among all the loads differently based on the individual load behavior. The UFLS schemes designed in this direction

usually include only one shedding step of the size equal to the estimated power deficiency for simplicity in analysis.

2.2.2 **Step-Oriented Adaptation**

Reference [27] introduces a method to adjust the shedding steps from the total available system spinning reserve. It has the advantage of simplicity. But the algorithm assumes that all the generators, including the lost ones and the undisturbed ones, have the same fraction of rating power as the spinning reserve. This may not always hold true in real power systems because generators' power rating and working condition may vary with time and space.

Reference [28] proposed a phase-plane based method to visualize the system status for designing the UFLS scheme and coordinating with speed governor control. The phase plane consists of frequency and ROCOF as the two dimensions and a calculated boundary which indicates whether a system status on the phase-plane needs to proceed load shedding or not. The paper shows that the scheme withstands a test of a series of losses of generation and has been implemented in practice.

Another adaptive UFLS schemes are proposed in reference [29], where the combination of frequency and ROCOF as an indicator for load shedding step adaptation is used. Results show that the scheme is viable for large penetration of renewable energy resources.

Several other novel UFLS scheme are proposed using various methods to make the load shedding steps more adaptive. For example, the authors of [30] proposed an adaptive UFLS scheme that involves fuzzy logic in distribution system. Reference [31] proposed a curve-based load shedding decision mechanics using frequency and voltage of local load to determine whether the system status satisfies the next shedding step. In reference [32] the second derivative of frequency is used to predict the frequency behavior.

In the present thesis, the scheme proposed in [24], i.e. the step adaptation based on the change of rate of change of frequency (ROCOF) is modeled and implemented in detail as a representative of the advanced, step-oriented UFLS. The implementation process and simulation results are shown in chapter 4.

2.2.3 **Topology-Oriented Adaptation**

While some advanced UFLS schemes assume that all the involved loads shed the same amount (percentage) on each frequency threshold, some others are designed to focus on the individual behavior of each load. A major common characteristic in these schemes is that there is only one step and only one set point, which simplifies the analysis. The main idea of the topology-oriented adaptation is that the calculated total shedding amount should be distributed in such a way that the loads with shorter distance to the disturbance location, which is reflected in different voltage or frequency behavior, should be cut off by a larger proportion, so that the spreading of the disturbance can be prevented and pre-fault power flow can be maintained.

Different topology-oriented adaptation methods have different ways to decide the distance between each load and the disturbance location. But the principle involved in the calculations is generally the same. The principle is expressed in equation (2-7) which shows what the schemes have in common during the adaption process.

$$P_{shed,i} = \frac{K_i}{\sum_i^{N_L} K_i} P_{shed} \tag{2-7}$$

where $P_{shed,i}$ is Shedding amount of ith load [MW]
P_{shed} is Total shedding amount [MW]
K_i is Distribution factor

With the total shedding amount that is pre-determined from the power deficiency estimation, each topology-oriented adaptation method has its unique algorithm to evaluate the distribution factor K_i.

For example, reference [32] uses the frequency deviation to distribute load shedding amount, as expressed in equation (2-8).

$$K_i = \Delta f_{Li} P_{L0i} \tag{2-8}$$

where Δf_{Li} is Frequency deviation of ith load immediately after the disturbance [Hz]

P_{L0i} is Pre-fault active power of ith load

In reference [33], the distribution factor is assumed to be directly the voltage deviation immediately after the disturbance.

$$K_i = \Delta V_{Li} \tag{2-9}$$

The author in reference [34] uses a so-called voltage reactive power sensitivity (VQS) as the distribution factor, which is shown in equation (2-10).

$$K_i = \frac{\Delta V_{Li}}{VQS_i} \tag{2-10}$$

where VQS_i is Voltage reactive power sensitivity factor at ith load

In reference [35], the pre-fault active power contribution of the lost generators to a load is used.

$$K_i = \Delta f_{Li} P_{tracing,i} \tag{2-11}$$

where $P_{tracing,i}$ is Pre-fault total active power at ith load bus received from the tripping generators

Among these considered topology-oriented adaptation UFLS schemes, the VQS method and power flow tracing method will be modeled and implemented in detail in chapter 5.

3 Methodology

Chapter Summary: In this chapter, the basic implementation aspects of advanced UFLS are introduced. Firstly, the software environment is introduced. Secondly, the implementation process in PowerFactory using Python is described in detail along with four sub-processes. Finally, the main assumptions involved in the implementation are discussed.

3.1 Simulation Environment

3.1.1 Software

The implementation of advanced UFLS schemes are processed in DIgSILENT PowerFactory. To verify the performance in a wider range of disturbance scenarios, multiple outage events are created in the software, thus Python is used to achieve a more dynamic and flexible implementation. During the implementation, Python sends commands, such as creating study cases, executing load flow (LDF) and RMS simulations, to PowerFactory. Then PowerFactory proceeds necessary calculations and writes data to csv files, which is later read by Python for graphical output. Figure 3-1 shows this interaction between PowerFactory and Python.

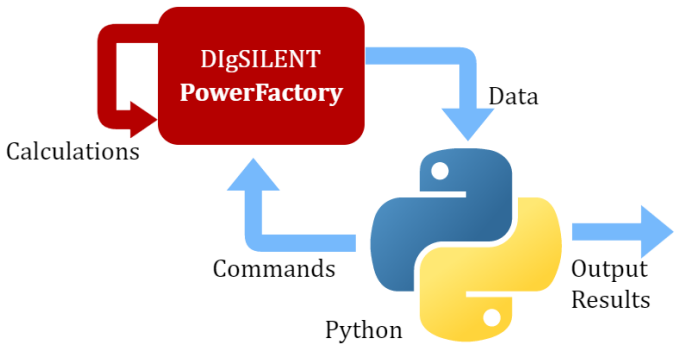

Figure 3-1: Python and PowerFactory Interaction for the Implementation

3.1.2 IEEE 39-Bus Test System

The UFLS schemes are implemented in the IEEE 39-bus test system [36], as shown in Figure 3-2. During the implementation, various system separation scenarios are created to form islands with generation deficiency.

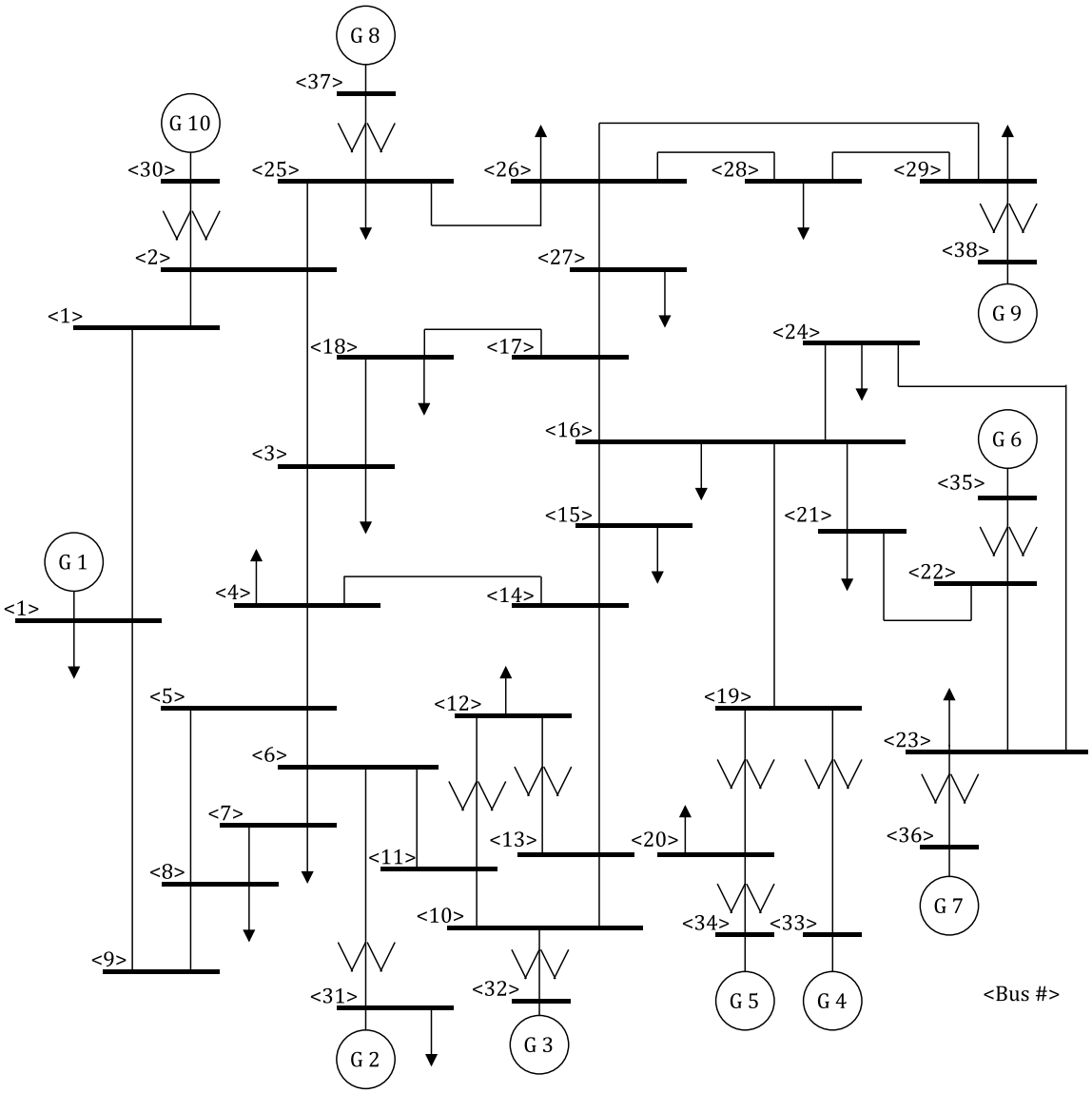

Figure 3-2: IEEE 39-Bus Test System

3.2 Implementation Process

The general implementation process is described graphically in Figure 3-3, which includes four sub-processes. These sub-processes serve the purpose of the preparation stage for the UFLS verification.

As the input of the program, outage events are designed to be user-defined for two reasons. First it can mimic the randomness and unpredictability of power system disturbances. Second the island topological information can be gathered from the outage event prior to the real verification stage, which can mimic the instant accessibility of topological data of real power system.

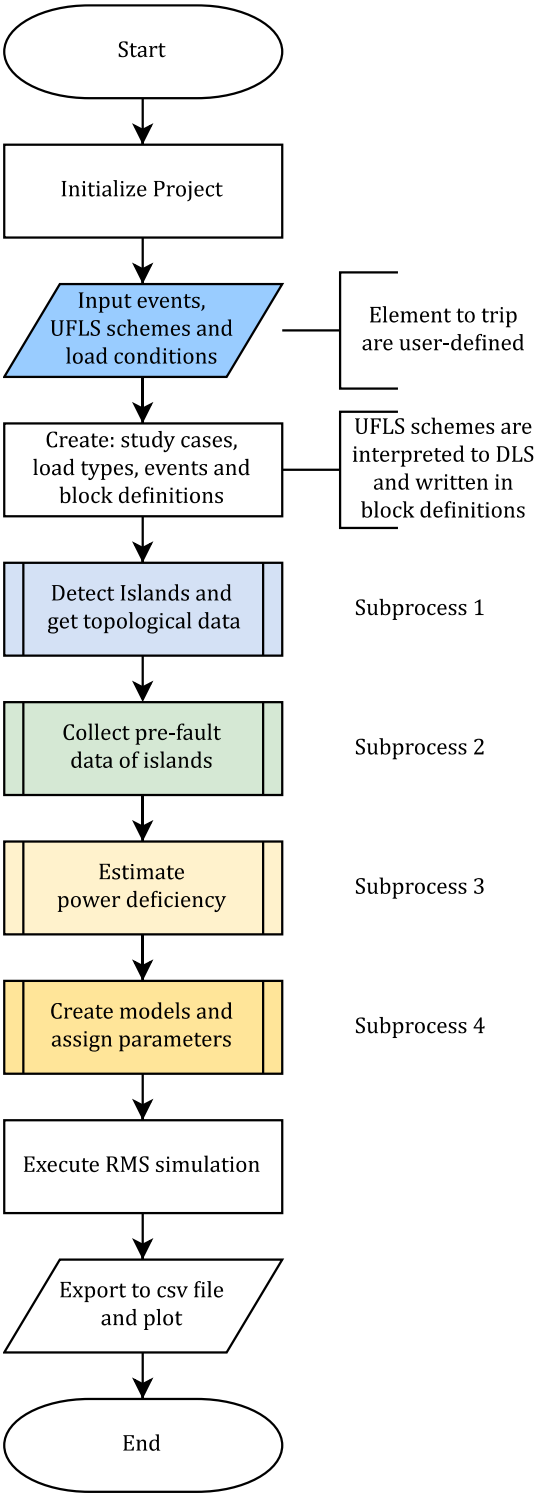

Figure 3-3: Implementation Process of Advanced UFLS Schemes

3.2.1 Sub-process 1: Detect Islands and Extract Topological Data

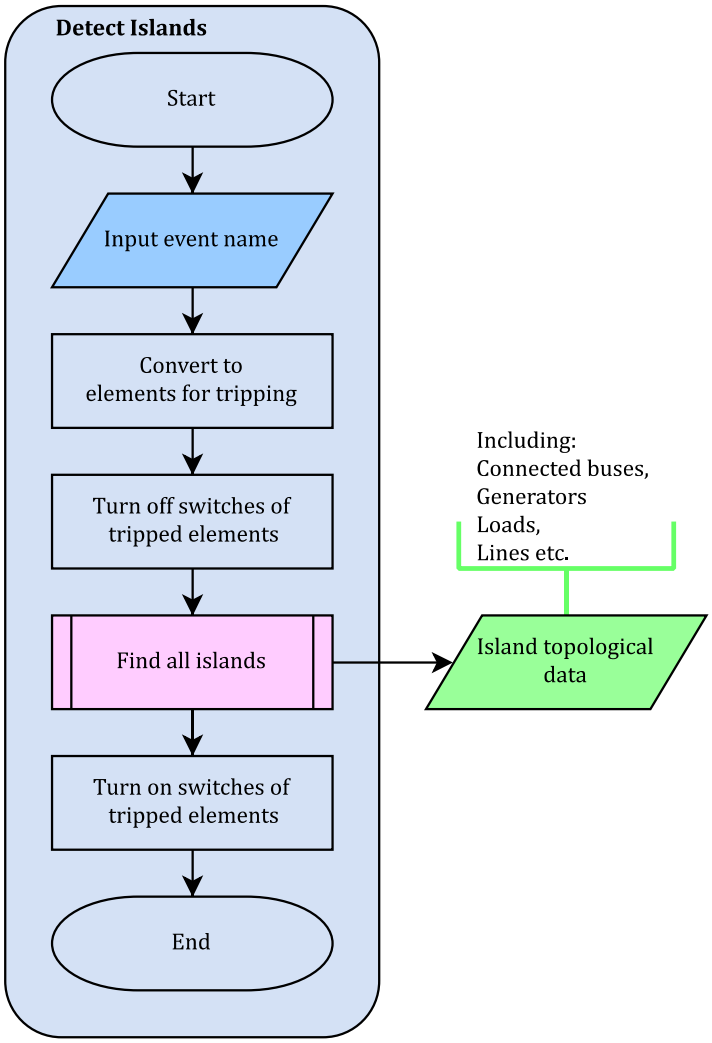

Figure 3-4: Sub-process 1: Detect Islands and Extract Topological Data

Before simulating UFLS schemes, the post-fault topological information of the system is unknown. In practice, island detection is done by the control center using data from PMUs [35]. To imitate this function, the program includes two switch manipulation steps, between which the system is manually separated and islands are found by a Python program.

The topological data generated from this sub-process is then passed to the second sub-process for collecting pre-fault data of elements that belong to the detected islands.

3.2.2 Sub-process 2: Collect Pre-fault Data

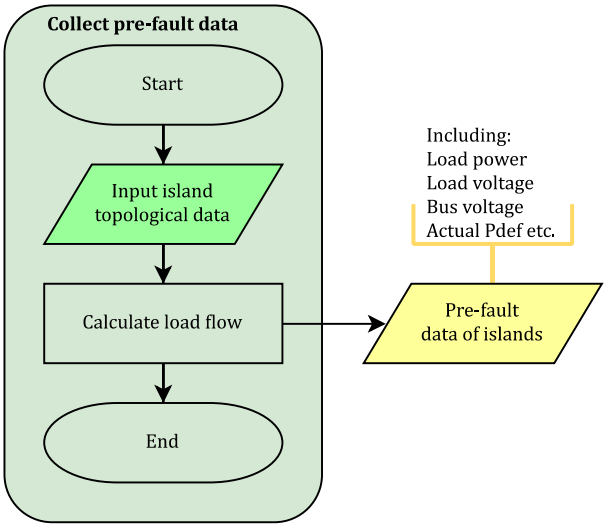

Figure 3-5: Sub-process 2: Collect Pre-Fault Data

In sub-process 2 a load flow calculation is executed for collecting pre-fault data, which includes active and reactive power of generator bus and load bus. The actual power deficiency is also calculated for later comparison.

3.2.3 Sub-process 3: Estimate Power Deficiency

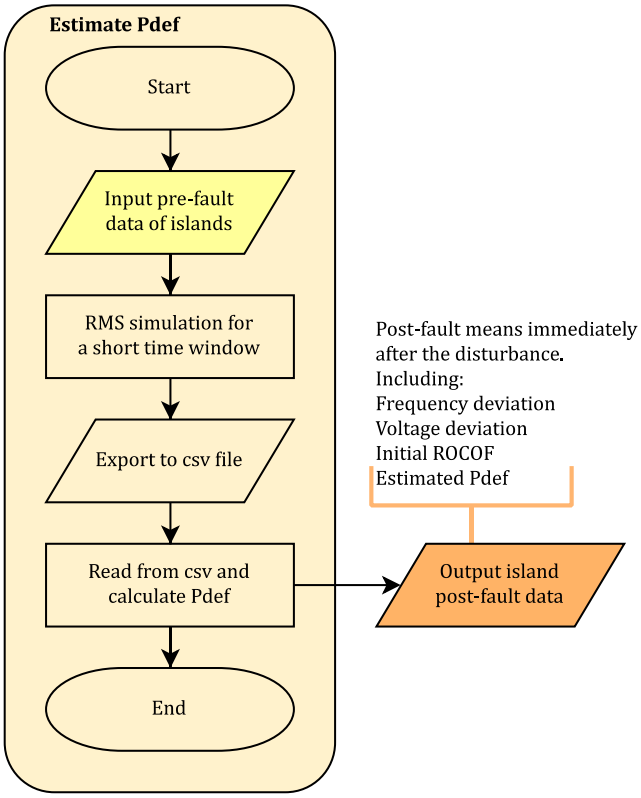

Figure 3-6: Sub-process 3: Estimate Power Deficiency

The third sub-process contains a short simulation for 3 seconds that serves the purpose of getting post-fault data of the island from a time window. Here, post-fault data means the load voltage and ROCOF value immediately after the disturbance that is assumed to be instantly accessible in real power system with the help of phasor measurement units (PMU).

Using equation (2-4), power deficiency can be estimated along with the initial ROCOF value, which is the lowest recorded value in the time window, and the voltage deviation, which is extracted at the end of the time window when voltage deviation is settled down. Figure 3-7 shows an example plot of the time window during the estimation stage.

Because ROCOF is calculated using the backward derivative in PowerFactory, the ROCOF curve is one calculation period (0.01s) delayed compared to the COI frequency signal.

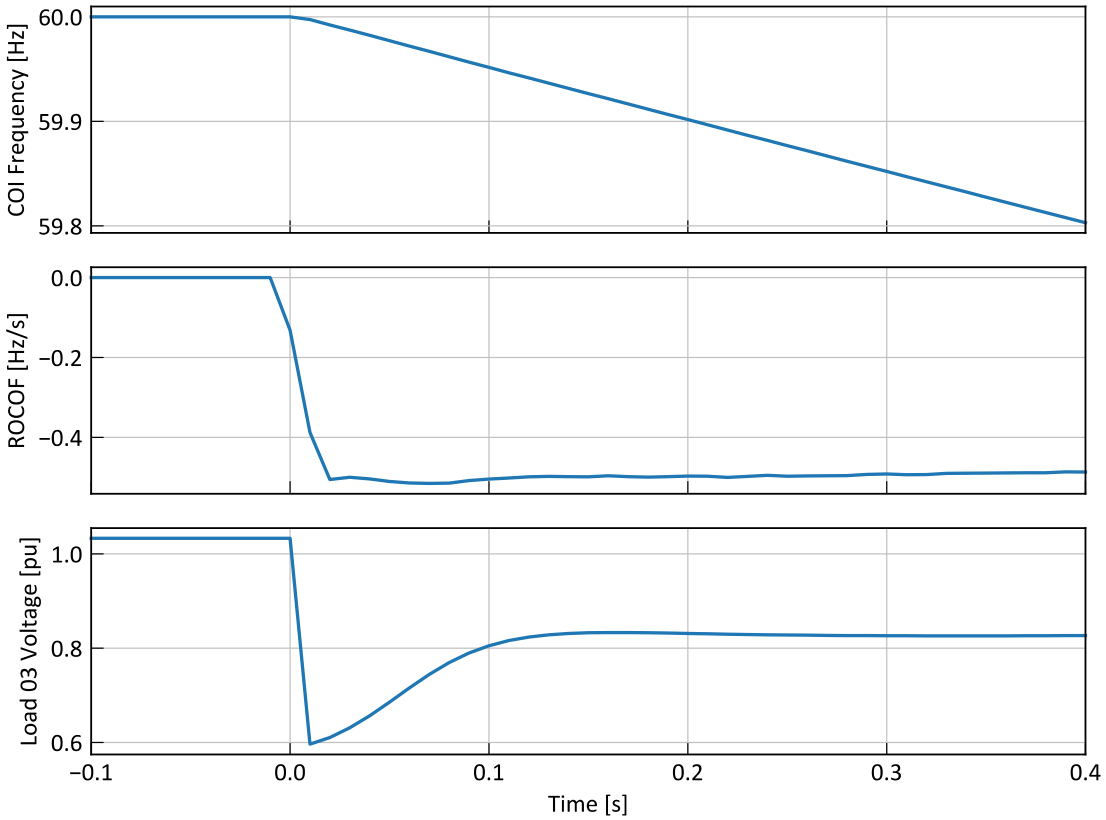

Figure 3-7: An Example Estimation Time Window

Here, the length of the time window is 0.4s for imitating the calculation delay in practice.

Figure 3-8 shows the estimation error after the simulation of four different outage events and three different load conditions. As will be mentioned in section 3.5, it assumes that all loads have the same power dependency on voltage in order to have a better observation on this estimation process. In addition, the estimation error is calculated using the following equation.

$$\text{Error} = \frac{P_{def}(Estimated) - P_{def}(Actual)}{P_{def}(Actual)} \times 100\%$$

From the results, it can be observed that:

1. The estimation method is in general accurate in various situations.
2. Larger α value leads to smaller error. This is because a larger α reflects a stronger dependency of load power on load voltage. When a disturbance occurs, the electrical frequency decreases along with load terminal voltage. Larger α can result in a larger load power decrease due to that voltage decrease, which temporarily mitigate the power imbalance, thus making the estimated P_{def} relatively smaller.
3. When α is equal to 0, the estimation method can be considered as a simplified version of equation (2-4), i.e. the following equation without considering load characteristics.

$$P_{def} = \frac{2H_{sys}S_{sys}}{P_{L0}f_n}\frac{df_{COI}}{dt} \tag{3-1}$$

Under this circumstance, the estimation error becomes as large as 8%. This observation further confirms the advantage of introducing load power dependency on voltage into the estimation process.

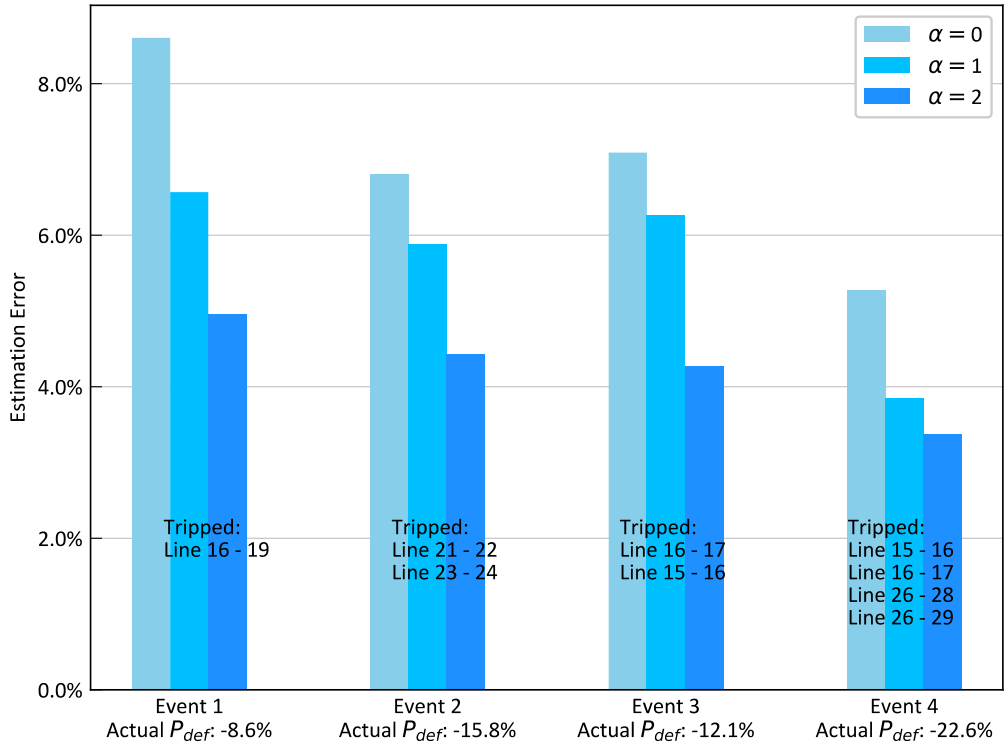

Figure 3-8: Simulation on the Accuracy of Power Deficiency Estimation

3.2.4 **Sub-process 4: Create Models and Assign Data**

Using the data obtained previously, models can be created following the sub-process 4 as shown in Figure 3-10. Figure 3-9 shows an example block diagram created in PowerFactory. In the example the UFLS scheme is implemented on an island that consists of three generators and three loads.

At the start of the diagram, generator speed, instead of electrical frequency at the machine terminal, is used as the frequency signal because the electrical frequency does not well represent mechanical speed of the generator during transient phenomenon [24].

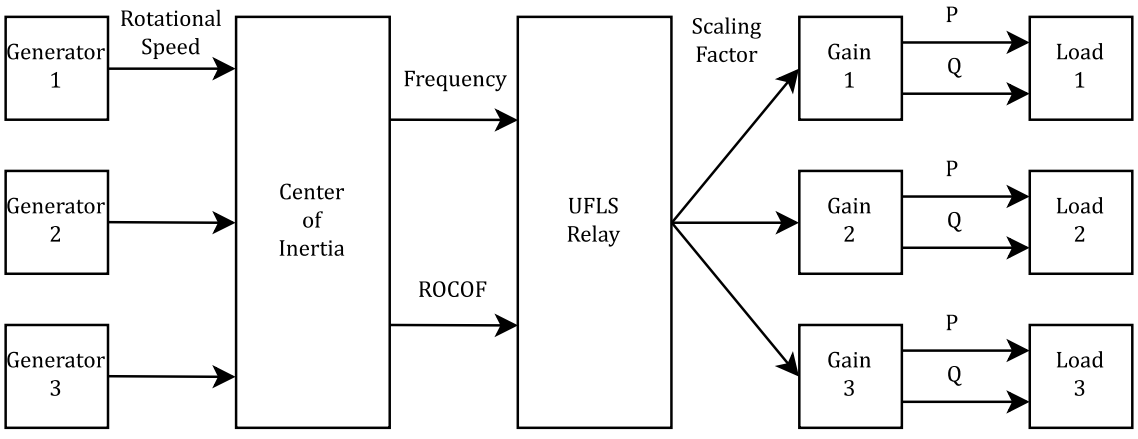

Figure 3-9: Example Block Diagram of a UFLS Scheme for 3 Generators and 3 loads

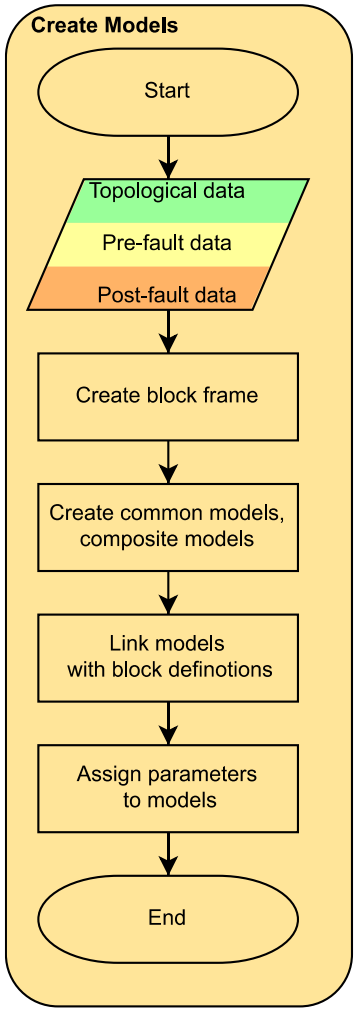

Figure 3-10: Sub-process 4: Create Models and Assign Data

The speed signals are gathered at a center of inertia (COI) block to calculate an average frequency of the whole island using the following equation.

$$f_{COI} = \sum_{j=1}^{N_G} f_j H_{j,eq} \tag{3-2}$$

$$H_{j,eq} = \frac{H_j S_j}{\sum_{j=1}^{N_G} H_j S_j}$$

where H_j is Inertia constant of jth generator based on its own rated capacity [s]

$H_{j,eq}$ is Equivalent inertia constant of jth generator based on the system rated capacity [s]

S_j is Apparent power of jth generator [MVA]

f_j is Frequency measured from speed of jth generator [Hz]

N_G is Number of generators in the system

Along with ROCOF, COI frequency is then sent to the relay block to calculate the scaling factor according to different UFLS schemes. Finally, the scaling factor is delivered to the load and converted to the power consumed by each load.

3.3 PowerFactory Models

3.3.1 Dynamic Load Model

Considering the assumption that load power dependency on frequency is ignored, dynamic load model in PowerFactory is simplified as shown in Figure 3-11. The value t_1 is the load dynamic time constant which is 0.1s by default.

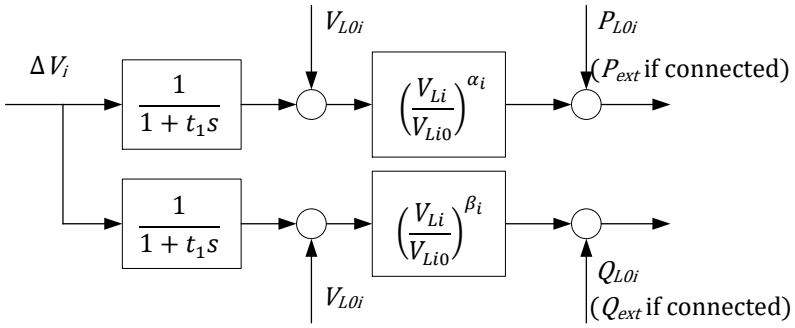

Figure 3-11: Simplified PowerFactory Dynamic Load Model

3.3.2 Load Gain Model

In the developed models, two signals P_{ext} and Q_{ext} are calculated from the load gain models, which is shown in Figure 3-12.

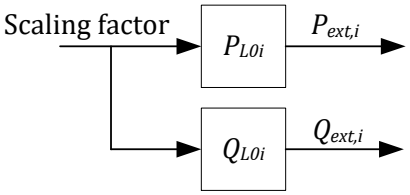

Figure 3-12: Load Gain Block Diagram

This block serves the purpose of proceeding the load shedding actions. The input signal scaling factor indicates what fraction of the pre-fault load power is remaining. The product of scaling factor and pre-fault power is the actual power consumed by the load. For example, scaling factor changes from 1 to 0.9 at a time instance means 10% load is curtailed as a shedding step.

3.3.3 UFLS Relay Model

As several advanced UFLS schemes are implemented, the detailed model of each UFLS relay will be shown respectively in the following chapters.

3.4 Implementation Objective

In the following chapters, several advanced UFLS schemes are modeled and implemented. To verify their performance and set an evaluative criterion, the IEEE UFLS objectives in [37] are used in the thesis as the main implementation objective. There are two goals for the frequency recovery for a generation deficiency of up to 25% of the load.

1. Frequency reaches no less than 58.5Hz in 10 seconds;
2. Frequency reaches no less than 59.5Hz in 30 seconds.

A UFLS scheme can be considered satisfactory if both goals are met under the specified operation condition and outage events without violating system stability. In addition, a UFLS scheme can be considered improved if the total shedding amount is reduced while remaining compliant with the IEEE guidelines.

3.5 Assumptions and Discussions

During the implementation process in chapter 4 and 5, there are several assumptions considered and discussed as follows.

1. Frequency is measured from generator rotational speed.

   As introduced in section 3.2.4, the frequency signal used in the implementation is obtained from generator rotational speed rather than terminal voltage. The purpose is to mitigate the influence induced by transient and sub-transient phenomena. As there appears various technologies in monitoring generator shaft speed at a high accuracy and linearity [[38],[39][40]], this assumption can be regarded as valid.

2. Center of inertia is used to evaluate the average frequency in the island.

   The calculation method is expressed in equation (3-2). Since many advanced UFLS schemes are based on a centralized control system, an average frequency is necessary to represent the behavior of the whole island. Individual frequency swing of a generator from the average frequency reflects the power imbalance of that generator, which is weighted by the equivalent inertia constant of the machine, as can be seen in equation (3-2).

3. Generator inertia constant is time-invariant.

   Inertial constants of generators may vary according to the operation status and the kinetic energy stored in the turbine. However, the time from the detection of frequency decay to protection action taken by UFLS relays is usually within 0.3 second [35]. Because synchronous turbines have a relatively large time constant, it is acceptable to assume the inertia constant to be time-invariant during the emergency control process.

4. Load characteristics are time-invariant and frequency dependency is negligible.

   For the same reasons as mentioned above, load characteristics can also be considered constant. Besides, active and reactive power of induction machines usually depend on terminal frequency. However, the estimation of power deficiency is based on ROCOF immediately after the disturbance, rather than frequency itself. Even though in practice there is unavoidable delay time of control and measurement system, frequency decrease is generally negligible during a measurement interval. Therefore, load frequency dependence is neglected in the thesis.

5. All loads have the same characteristics, i.e. power dependency on voltage.

   In practice power system loads have different characteristics. As mentioned in section 2.2.1, both α and β vary in certain ranges. But the thesis assumes a uniform factor have a better observation of the impact of load dynamics on UFLS performance. Nevertheless, to imitate the real variation of load dynamics, random α are assigned to the load models during the implementation in the following chapters.

6. All loads are equally and continuously reducible.

   To investigate and verify the performance of selected UFLS schemes, the assumptions are made throughout the following implementation to avoid impact of other factors such as load priority, even though this may not hold in practice and should be adjusted accordingly.

7. The length of time window as 0.4s can be justified.

As the first frequency threshold is selected to be 1% lower than the rated value, the time window should not be so long that the first threshold has already been reached when the estimation process is ended. Besides, a security margin should be applied. During the implementation, the margin is chosen to be 0.3Hz, meaning that at the end of the time window the COI frequency should be above 59.7Hz.

$$T_{TW} ROCOF_{min} \leq 0.3\text{Hz}$$

Here T_{TW} is the length of time window in seconds. For simplicity, load power dependency on voltage is ignored. Combining equation (2-4), the following relation can be obtained.

$$\frac{P_{def} P_{L0}}{2 H_{sys} S_{sys}} T_{TW} \leq 0.005$$

Considering the IEEE guideline which indicates that the power deficiency dealt with UFLS can be up to 25% of the total pre-fault load power, the maximum T_{TW} is expressed using the above equation as

$$T_{TW} \leq \frac{H_{sys} S_{sys}}{25 P_{L0}}$$

Although the value of $H_{sys} S_{sys}$ and P_{L0} vary according to different island topology, the simulation results of multiple events show that the maximum T_{TW} is generally greater than 0.5s. For example, in the four events in Figure 3-8 the values are calculated as 0.56s, 0.53s, 0.62s, 0.66s, respectively. Considering the safety margin of 0.3Hz, the length of time window of 0.4s can be considered valid.

4 Implementation of Step-Oriented UFLS

Chapter Summary: In this chapter, an advanced UFLS scheme that uses $ROCOF$ to dynamically adjust load shedding step is selected and implemented. First the load shedding principle and mechanics are introduced. Then the scheme is implemented in several separation scenarios to verify the performance with various influential factors such as the load characteristics. Finally, a step correction method is proposed in order to improve the load shedding effectiveness.

4.1 Introduction

Chapter 2 introduces several state-of-the-art step-oriented UFLS schemes. Based on an accurate power deficiency estimation, these schemes distribute the shedding amount to each step in various ways while making all the loads disconnect the same percentage when a step takes place. To develop a set of PowerFactory models for general implementation, it is necessary to choose one scheme as a base that has the following features.

1. Sufficient flexibility for a wider range of operating conditions. The scheme should be useful for multiple systems and disturbance scenarios.
2. Appropriate compatibility in PowerFactory. Implementation of the scheme should be well supported by available PowerFactory functions and models.
3. Extendibility to other UFLS schemes. With minor change in certain block definitions the set of models can be suitable for implementation of another scheme.

For the above reasons, the scheme proposed in reference [24] is selected to be modeled in the IEEE 39-bus system to verify its performance under different operation conditions.

The principle of this scheme is that, along with UFLS, speed governor and other controllers contribute to the power balance recovery as well. During the interval of two steps, these controllers may have already recovered certain amount of power that results in the increase of $ROCOF$. This increase is recorded and converted to the reduction of the subsequent step so that the total shedding amount is minimized.

Same as in other advanced UFLS, the initial total shedding amount is the estimated power deficiency. Even if there is no available spinning reserve ($ROCOF$ does not increase before a step), the under-frequency relay can still disconnect the initial shedding amount, leading to the elimination of power imbalance. Detailed mechanics are described below.

4.2 Load Shedding Mechanics

According to [24], UFLS relays is configured immediately after the power imbalance estimation stage. Necessary parameters for the relay configuration are shown in Table 4-1.

Table 4-1: Configuration Parameters for the UFLS Relay Model

Parameter	Type	Unit	Description
$f_{th,i}$	Input	Hz	Frequency threshold of the ith step
P_{shed}	Input	1	Initial total shedding amount, equal to estimated power deficiency: $P_{shed} = P_{def}$
T_{delay}	Input	s	Time delay
$ROCOF_{min}$	Input	Hz/s	Recorded minimum $ROCOF$ within the time window
$P_{step,i}$	Input	1	Shedding amount of the ith step (as a fraction of the total shedding amount, the sum of all steps equals to 100%)
$P'_{step,i}$	Intermediate	1	Adjusted shedding amount of ith step*
Δ_i	Intermediate	1	Relative $ROCOF$ change before i th step (as a fraction of $ROCOF_{min}$)

As suggested in [24], the UFLS scheme uses four steps that bring the $ROCOF$ from the minimum value back to zero, assuming that the available spinning reserve in the system is sufficient to gradually recover the frequency to the nominal value after the load shedding steps.

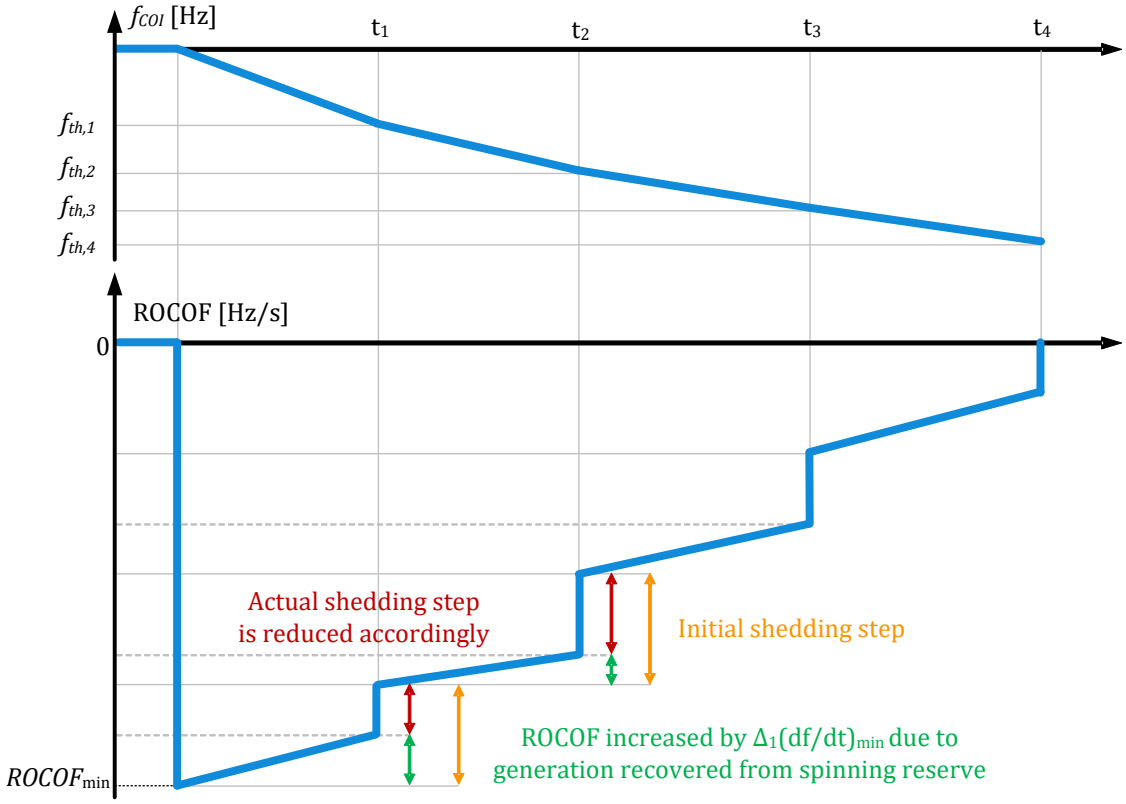

Figure 4-1: Illustrative Mechanics of the UFLS Scheme

1. At $t = 0$, a contingency occurs in power system and induces a power imbalance situation. The center of inertia frequency begins to decrease. Before the time window ends, the minimum ROCOF is captured by the control center.

2. At $t = t_1$, frequency drops to the first threshold $f_{th,1}$. Due to the power restored from spinning reserve, $ROCOF$ has increased by $\Delta_1 ROCOF_{min}$ before t_1.

3. Under-frequency relays are given the order to execute load shedding, but the shedding amount is re-calculated. Here the linear relation between $ROCOF$ and power imbalance is assumed, i.e.

$$ROCOF(t) \propto P_{def}(t) \tag{4-1}$$

Based on this assumption, the value Δ_1 that represents the relative change of $ROCOF$ increase can also reflect Δ_1 of power deficiency decrease because of the contribution of spinning reserve. Therefore, the first shedding step is adjusted accordingly, i.e.

$$P'_{step,1} = P_{step1} - \Delta_1.$$

It is noteworthy that two unexpected situations may occur. First, due to excessive frequency oscillation or other controller effects, the change in $ROCOF$ before the first step can be larger than the initial step. Thus, a limit is added to the equation to regulate the output signal.

$$P'_{step,1} = max\left(P_{step,1} - \Delta_1, 0\right) \tag{4-2}$$

Second, if the overload situation is aggravated, $ROCOF$ can further decrease, resulting in a negative change ($\Delta_1 < 0$). However, the adjusted step becomes larger than initial value and will bring the system to the safe side.

4. After a delay time T_{delay}, the first step takes place, making the $ROCOF$ rise to the value that is planned by the initial size of the first step.

$$ROCOF|_{t=t_1+T_{delay}} = \left(1 - P_{step,1}\right) ROCOF_{min} \tag{4-3}$$

5. The next three steps follow the same pattern to adjust the steps according to the $ROCOF$ change.

As the contribution made by spinning reserve is actively involved, the shedding amount at every step is no more than its planned value, making the overall shedding amount less than the actual generation deficiency.

4.3 Implementation in PowerFactory

The implementation of the UFLS scheme proposed in [24] is written in code using DIgSILENT Simulation Language (DSL) inside PowerFactory models. The input signal of the relay is center of inertia (COI) frequency and its first derivative. The output signal is the scaling factor that is sent to each load gain block. Detailed code that fully represents the load shedding mechanics is shown in appendix. Figure 4-2 is a graphical expression of the mechanics.

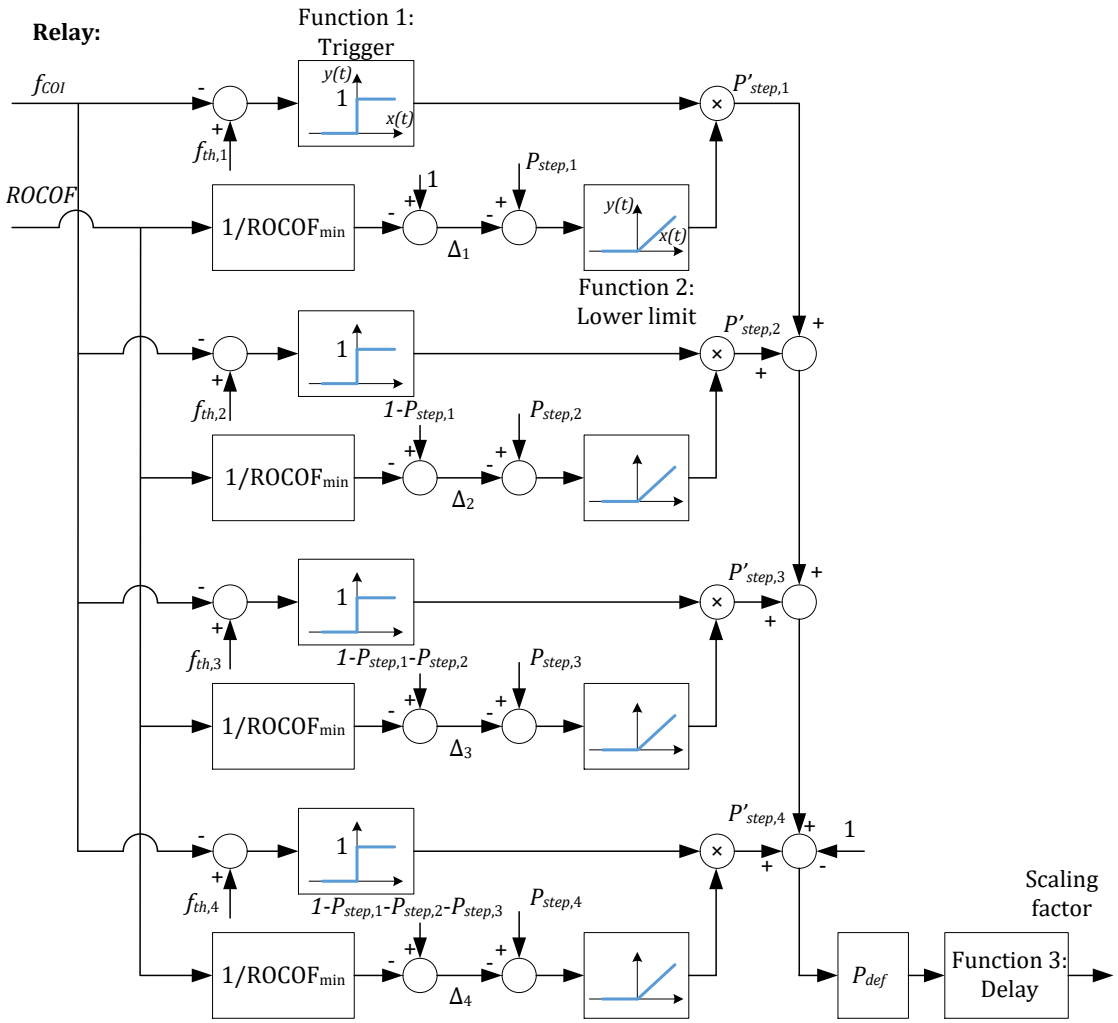

Figure 4-2: Graphical Mechanics of the UFLS Proposed in [24]

Some key functions in Figure 4-2 are described below. Here, the input and output of the functions are $x(t)$ and $y(t)$, respectively, where t is time.

1. Function 1: Trigger. This function is used as the decision stage whether the frequency has reached a threshold.

$$y(t) = \begin{cases} 0 & , x(t) < 0 \\ 1 & , x(t) \geq 0 \end{cases}$$

2. Function 2: Lower limit. This function is the same as equation (4-2).

$$y(t) = \begin{cases} 0 & , x(t) < 0 \\ x(t) & , x(t) \geq 0 \end{cases}$$

3. Function 3: Delay. This function imitates the delay time in a real control system. The initial value equals to 1 because the scaling factor starts at 1.

$$y(t) = \begin{cases} 1 & , 0 \leq t < T_{delay} \\ x(t - T_{delay}) & , \quad t \geq T_{delay} \end{cases}$$

During the implementation, it is observed that the performance of the UFLS scheme is affected by several factors, including load dynamic characteristics and under-frequency relay settings. Among them, the initial step size and the load power dependency on voltage have more significant impact on the frequency behavior. In the following sections these influential factors are investigated with simulation results.

4.4 Influential Factor: Initial Step Size

The first factor to be investigated is the initial shedding amount distribution within the four steps. As can be assumed, frequency decline should be stopped as soon as possible, thus the size of the first shedding step presumably has a significant impact on the frequency excursion. In [24], it is suggested to divide the estimated power deficiency equally into four steps, each of which accounts for 25% of the total shedding amount.

$$P_{step,1} = P_{step,2} = P_{step,3} = P_{step,4} = 25\%$$

To verify this step distribution, four different distribution cases are simulated and compared. Specific values are listed in Table 4-2 where $P_{step,i}$ is the percentage of the total shedding amount.

Table 4-2: Four UFLS Step Distribution Cases

	$P_{step,1}$	$P_{step,2}$	$P_{step,3}$	$P_{step,4}$
Case 1	100%	0%	0%	0%
Case 2	75%	15%	10%	0%
Case 3	50%	20%	15%	15%
Case 4	25%	25%	25%	25%

Other factors are temporarily assumed constant, as listed in Table 4-3. Two system separation scenarios of different magnitude of disturbance are created to form the islands where the UFLS scheme is implemented.

Table 4-3: Assumed Constant Values for Comparing Initial Step Sizes

Name	**Value**
Frequency thresholds $f_{th,2}, f_{th,2}, f_{th,3}, f_{th,4}$	59.4Hz, 59.1Hz, 58.8Hz, 58.5Hz
Delay time T_{delay}	0.3s
Active power dependency on voltage α	1
Reactive power dependency on voltage β	2

4.4.1 **Separation Scenario A: Two Transmission Lines Tripped**

The tripping of transmission line 15 – 16 and line 16 – 17, are created in PowerFactory as a disturbance, resulting in the actual P_{def} equal to -12.1% in one of the two islands, which is shown in Figure 4-3. Figure 4-4 shows the simulation results for comparing the four step distribution cases.

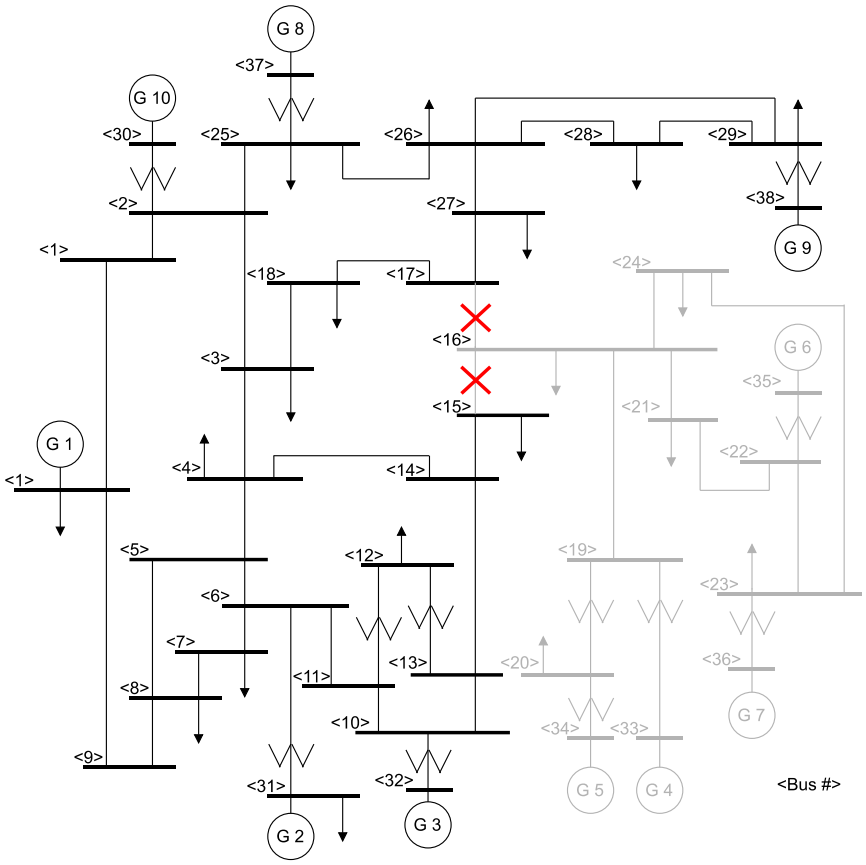

Figure 4-3: Separation Scenario A (Two Transmission Lines Tripped)

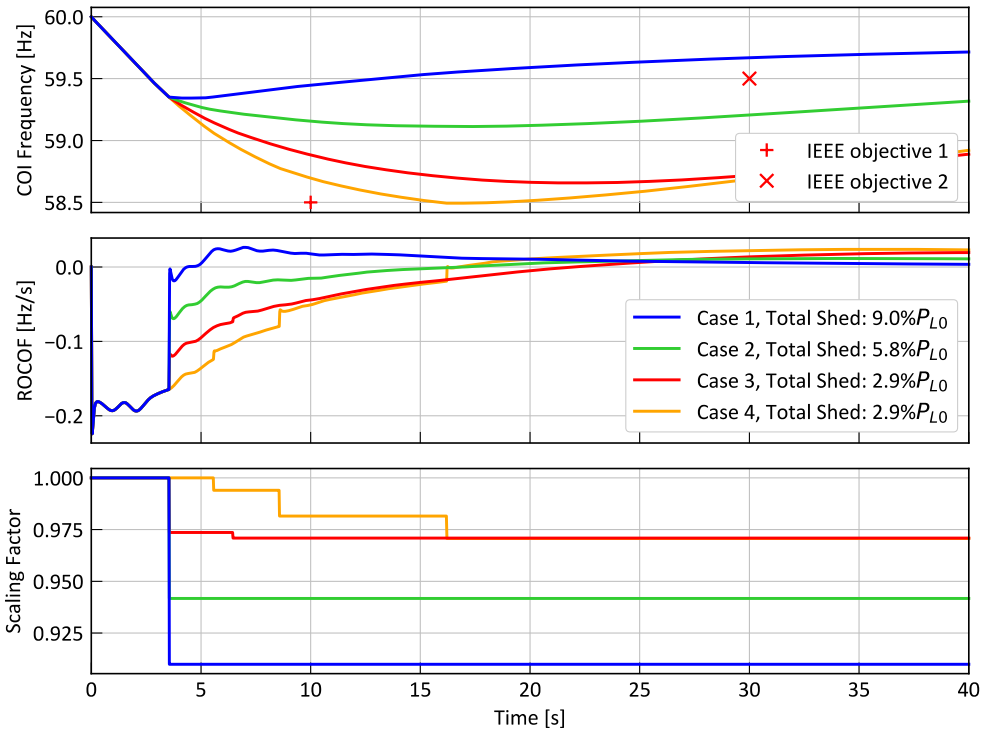

Figure 4-4: Comparing Four Distribution Cases in Separation Scenario A

From Figure 4-4, it can be observed that only when the initial step equals to P_{def} can the frequency recovery satisfy the two IEEE objectives. However, the other three cases can also successfully arrest

the frequency decline and have less total shedding amount. These step distribution cases can be considered valid if the UFLS objectives are less strict.

4.4.2 **Separation Scenario B: Four Transmission Lines Tripped**

For this scenario, four transmission lines, namely Line 15 – 16, Line 16 – 17, Line 26 – 28 and Line 26 – 29, are tripped to create a more severe separation as shown in Figure 4-5 and Figure 4-6. The disturbance causes a 22.6% as power deficiency of one of the three islands. Since the other two islands have generation surplus compared to the load, they are not considered here.

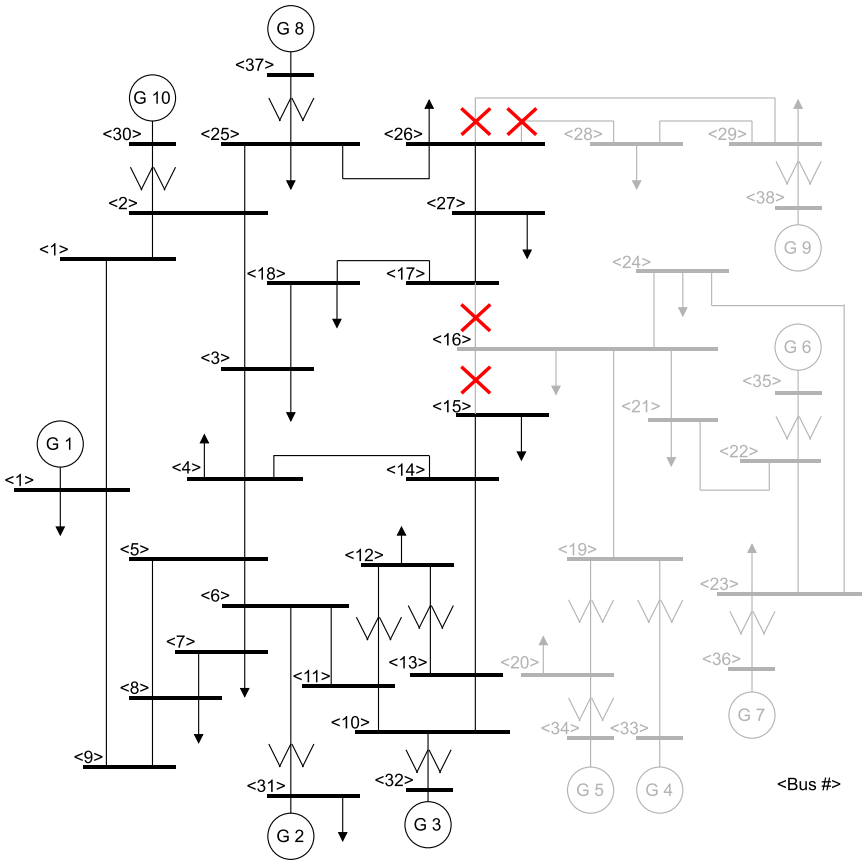

Figure 4-5: Separation Scenario B (Four Transmission Lines Tripped)

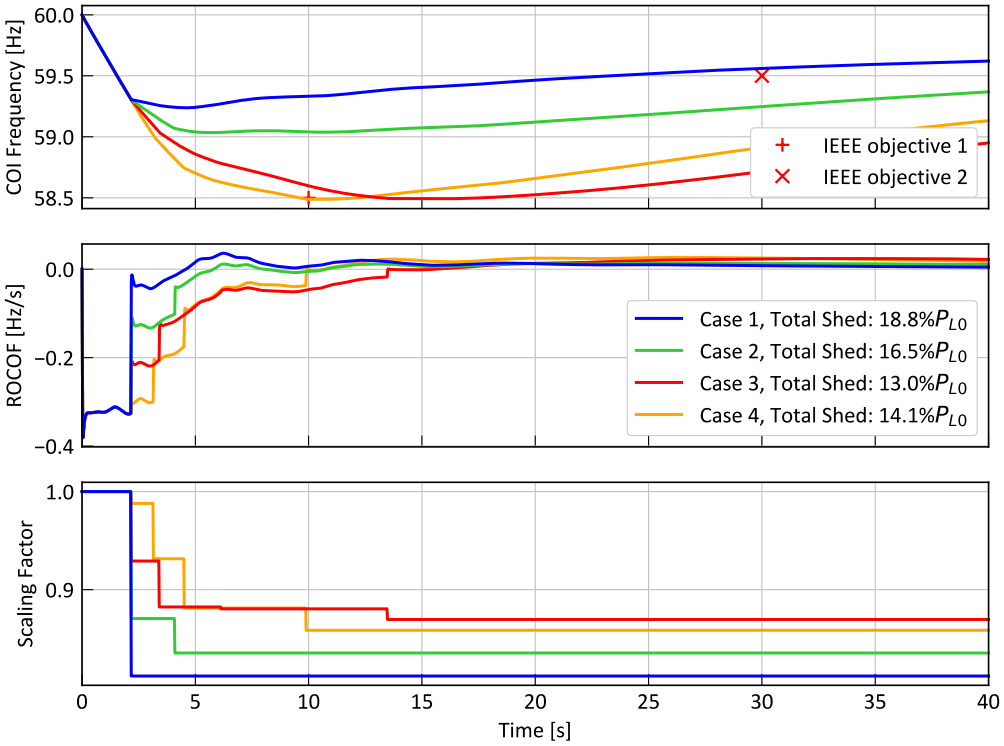

Figure 4-6: Comparing Four Distribution Cases in Separation Scenario B

Same as in scenario A, all four different step distribution cases in scenario B can successfully prevent the COI frequency from decreasing below 58.5Hz, but only case 1 can satisfy the IEEE objectives.

4.4.3 Conclusion on the Influence of Initial Step Size

From the previous investigation on the influence of initial step size, the following conclusions can be drawn.

1. In various step distribution cases, the UFLS scheme is in general successful in two ways. First, it can arrest frequency decline. The minimum value of COI frequency observed in the results is equal to the last frequency threshold, i.e. 58.5Hz. Second, the total shedding amount of the scheme is kept less than the actual power deficiency.
2. The initial step has a significant influence on the COI frequency behavior. A larger step, such as 75% or 100%, makes the frequency recovery faster, while a smaller step results in a slower frequency recovery. Only in case 1 can the COI frequency behavior satisfy both the IEEE objectives.
3. In terms of total shedding amount, a larger initial step leads to a smaller steady-state scaling factor, which means a larger load shedding percentage.

For simplicity in later implementation and analysis, the step distribution case 1 is chosen to be the step configuration of the UFLS scheme proposed in [24].

4.5 Influential Factor: Load Active Power Dependency on Voltage

In section 3.2.3 the estimation of power imbalance is proved to be accurate in various system separation events. However, the accuracy is influenced by the load active power dependency on voltage, i.e. α, which raises the necessity to investigate the impact of α on the overall load shedding process.

The same two events as in section 4.4 are simulated. Other parameters are also the same as in Table 4-3 except that the first shedding step is equal to the estimated power deficiency.

4.5.1 Separation Scenario A: Two Transmission Lines Tripped

Simulation result of COI frequency, ROCOF and the scaling factor is shown in Figure 4-7.

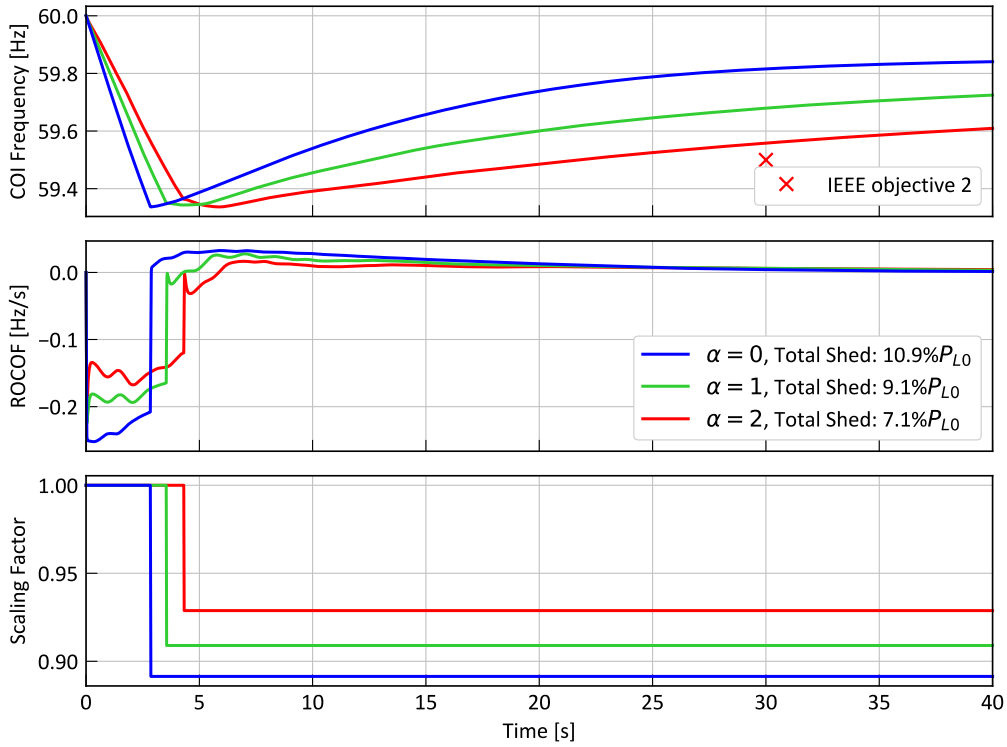

Figure 4-7: Comparing Load Power Dependencies on Voltage in Separation Scenario A

For different α values, the UFLS scheme operates well to prevent the frequency from decreasing and successfully recovers it to compliance with IEEE objectives.

Apparently, higher α leads to less shedding amount of the adjusted first step. This is because α reflects the connection between load voltage and load active power. A larger α means a stronger active power dependency on the terminal voltage, and can lead to a greater active power decrease when the voltage decreases. Immediately after the disturbance, load bus voltages drop to a certain level, and a larger α causes a larger reduction in load active power, which is seen by the UFLS relay as less severity of the power imbalance. According to the load shedding mechanics introduced previously, the shedding step is adjusted to be smaller when α is larger, causing the total shedding amount smaller.

4.5.2 Separation Scenario B: Four Transmission Lines Tripped

The second event, which is the same as in Figure 4-5, is simulated to strengthen the reasoning above that a larger value leads to a smaller shedding amount. Results are shown in Figure 4-8.

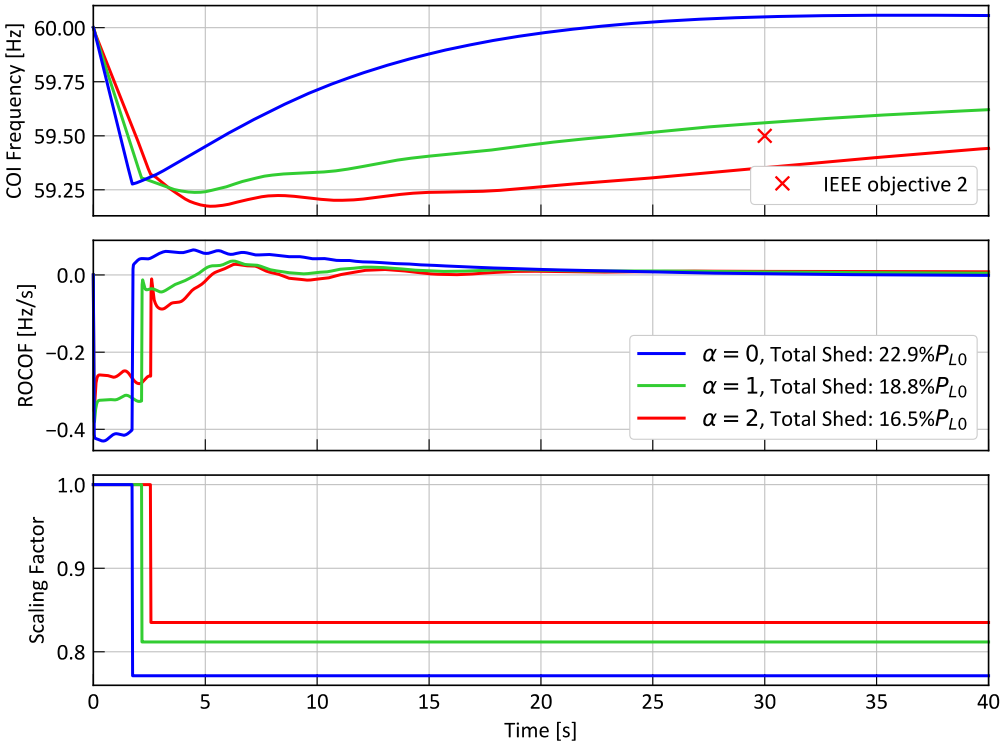

Figure 4-8: Comparing Load Power Dependencies on Voltage in Separation Scenario B

In this event where the power imbalance becomes worse, the previous conclusion that larger α leads to smaller shedding step is observed valid. Again, the total shedding amount is less than the actual power deficiency and the recorded minimum COI frequency is greater than 59Hz. Judging from this phenomenon, it can be concluded that the ability of the UFLS to arrest the frequency decline while reducing the total shedding amount does not depend on α value.

However, when α is equal to 2, the reduction of load active power due to the voltage decrease is so large that the shedding step is reduced to a level that is insufficient for UFLS relay to recover the COI frequency to compliance with IEEE goals, as can be seen from the red curve in Figure 4-8.

4.5.3 Conclusion on the Influence of Load Active Power Dependency on Voltage

In conclusion, load active power dependency on voltage does not affect the UFLS ability to rescue COI frequency, but it influences the load shedding performance in such a way that larger α results in less shedding amount and thus slower recovery of frequency. This phenomenon has a two-fold effect on frequency recovery behavior depending on the specific power imbalance scenario.

First, if the disturbance is relatively small, for example as in scenario A, less shedding amount means better performance while keeping the IEEE goals.

Second, if the disturbance is large, for example as in scenario B, less shedding amount may lead to an excessively small step that makes the frequency behavior not compliant with IEEE objectives.

As both α and P_{def} take part in frequency excursion for the UFLS scheme, in section 4.7 a correction method that takes these two parameters into account is proposed to improve the load shedding performance.

4.6 Other Influential Factors

The performance of UFLS schemes are affected by some other factors such as the relay setting and load reactive power dependency on voltage, i.e. β. Simulation results show that, although the impact exists, these factors have negligible influence on the overall frequency excursion. Different values generally lead to very similar results. Thus, they will not be further considered.

4.7 Load Shedding Step Correction

Previous implementation results have demonstrated the swing equation in a simulative way that the load shedding amount is a trade-off factor against frequency recovery. The more amount of load is disconnected at a step, the faster COI frequency can be recovered. As observed before, both α and P_{def} have significant impact on UFLS scheme performance. When the power system disturbance is small, a large α helps frequency recovery positively by decreasing the shedding amount without violating the IEEE objectives. But when the disturbance is large enough the reduced shedding amount can result in an overly-slow recovery of frequency that is incompliant with the IEEE objectives.

Based on this observation, the adjusted step mechanics can be further improved by taking α and P_{def} into account. The objective of this improvement is to re-calculate the initial step size during the power deficiency estimation stage and find a balance point between the trade-off factors, meaning that shedding amount is minimized while the IEEE objectives are satisfied. The formula is shown below in equation (4-4). After the recalculation, the new step size P'_{step1} is assigned to the relay model.

$$P'_{step1} = K_1 + K_2 P_{def} + K_3 \alpha + K_4 P_{def} \alpha \tag{4-4}$$

where K_1 is Off-set value as the basis of the shedding amount
K_2 is Effect of α, which represents the impact of system response
K_3 is Effect of P_{def}, which represents the impact of magnitude of disturbance
K_4 is Combined effect of α and P_{def}

A trial-and-error method is used to decide the value of each factor. As a result, the following setup is tested to be acceptable for effective correction in various simulated cases.

$$K_1 = 0.5, \qquad K_2 = 3.3, \qquad K_3 = 0.25, \qquad K_4 = -1.2$$

4.7.1 Testing Step Correction in Scenario A and B

The step correction method is applied to the UFLS schemes and verified in separation scenario A and B, as shown in Figure 4-9 and Figure 4-10, respectively. It can be observed that in both situations the corrective method is effective in improving the frequency performance for different α values. Compared to the uncorrected step, the new step is better in terms of finding the balance point in the trade-off between reducing shedding amount and satisfying the IEEE objectives.

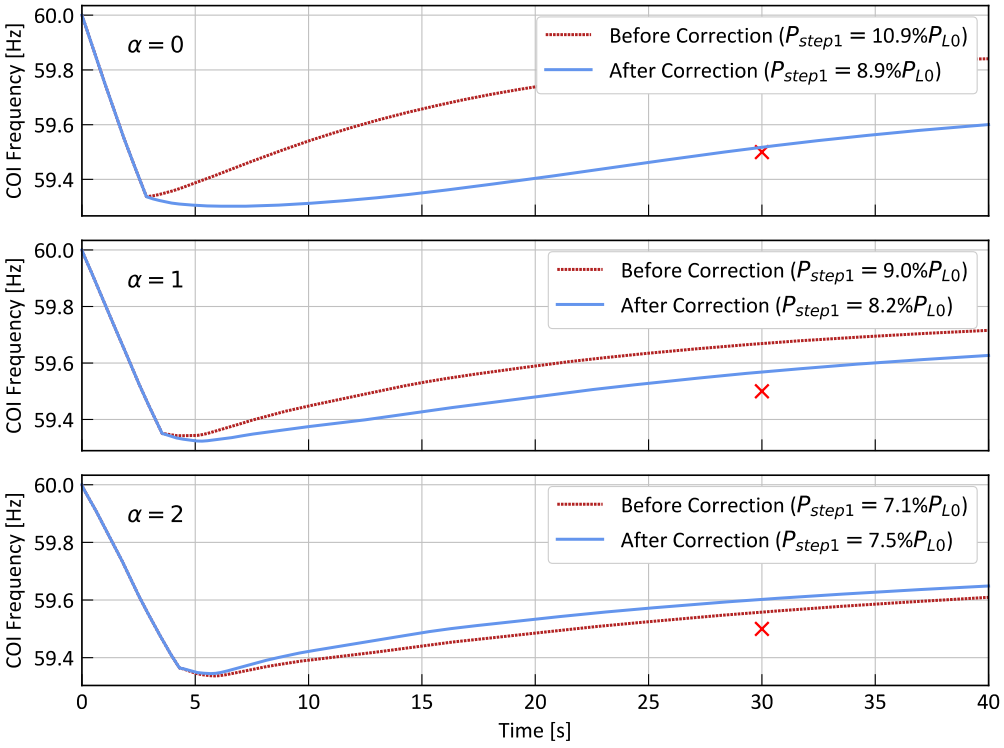

Figure 4-9: Testing Step Correction in Scenario A

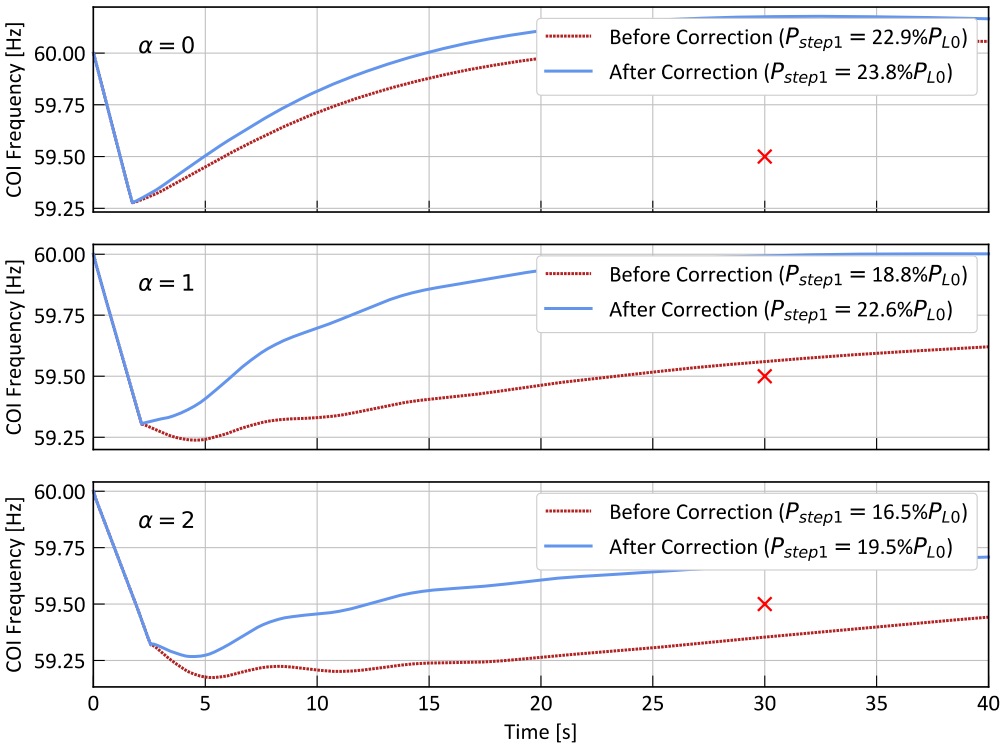

Figure 4-10: Testing Step Correction in Scenario B

4.7.2 **Testing Step Correction in Scenario C and D**

To verify the validity of the correction method, another two separation scenarios are created. In scenario C, as shown in Figure 4-11, the actual power deficiency is -8.6%. In scenario D, as shown in Figure 4-13Figure 4-11, the actual power deficiency is -22.6%. Results are shown in Figure 4-12 and Figure 4-14.

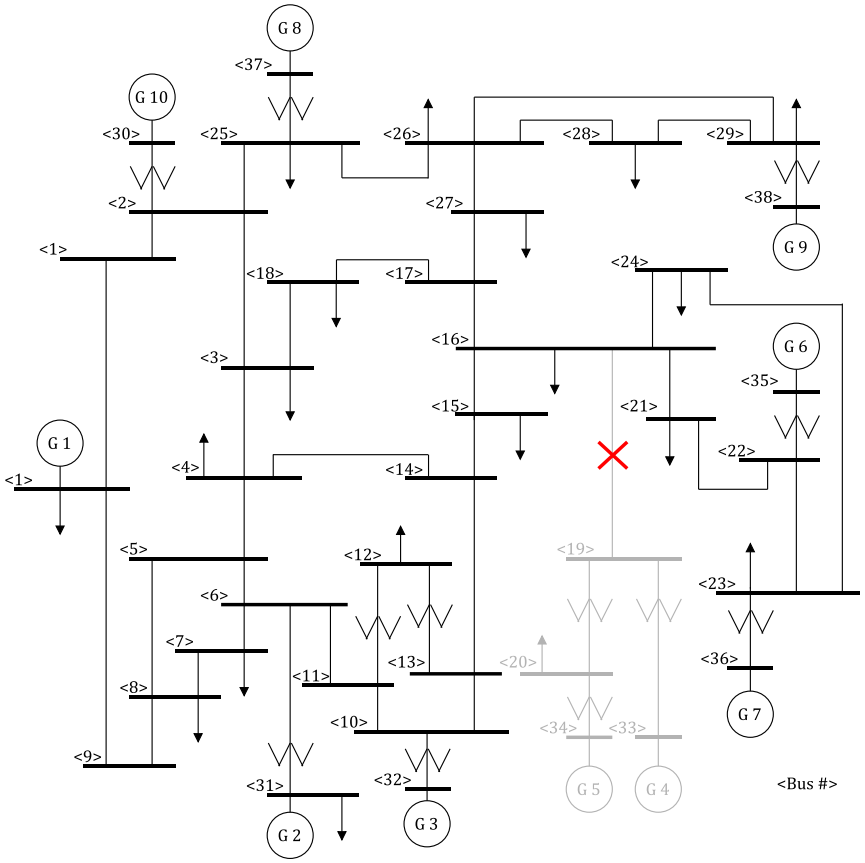

Figure 4-11: Separation Scenario C (One Transmission Line Tripped)

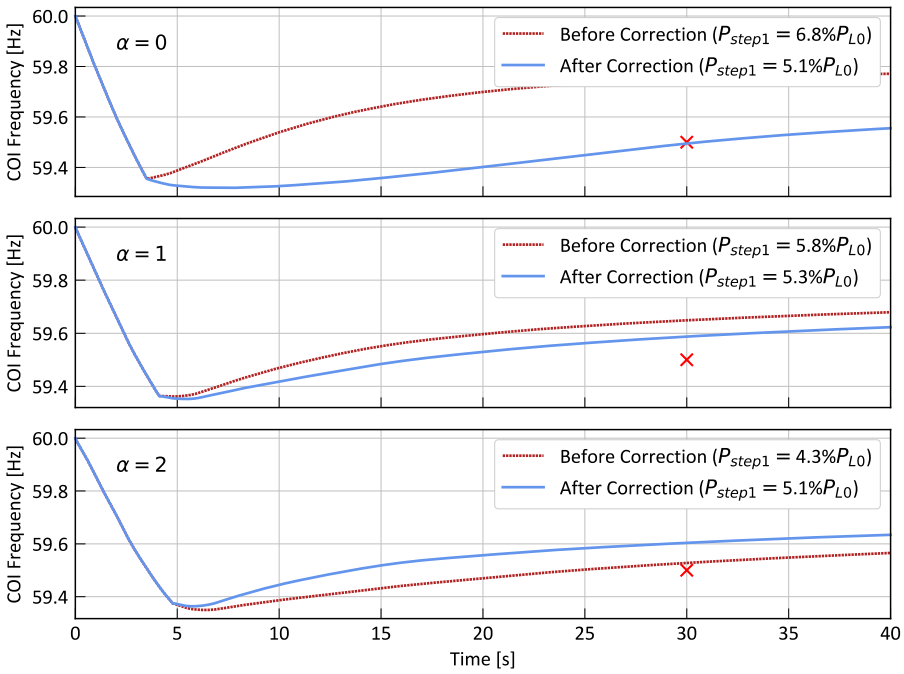

Figure 4-12: Testing Step Correction in Scenario C

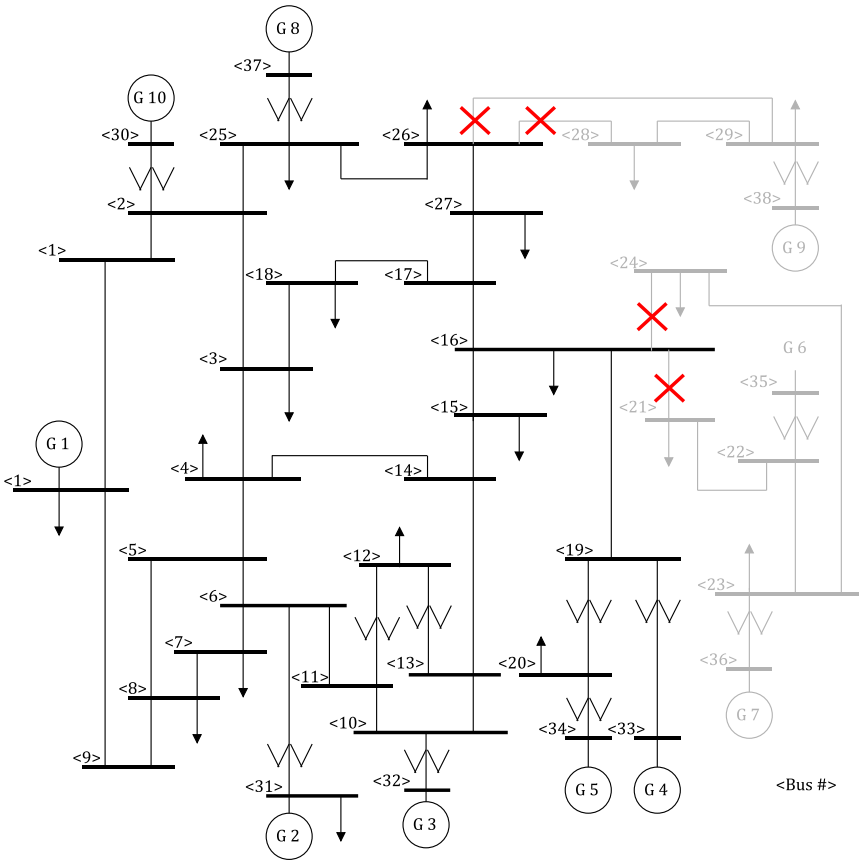

Figure 4-13: Separation Scenario D (Four Transmission Lines Tripped)

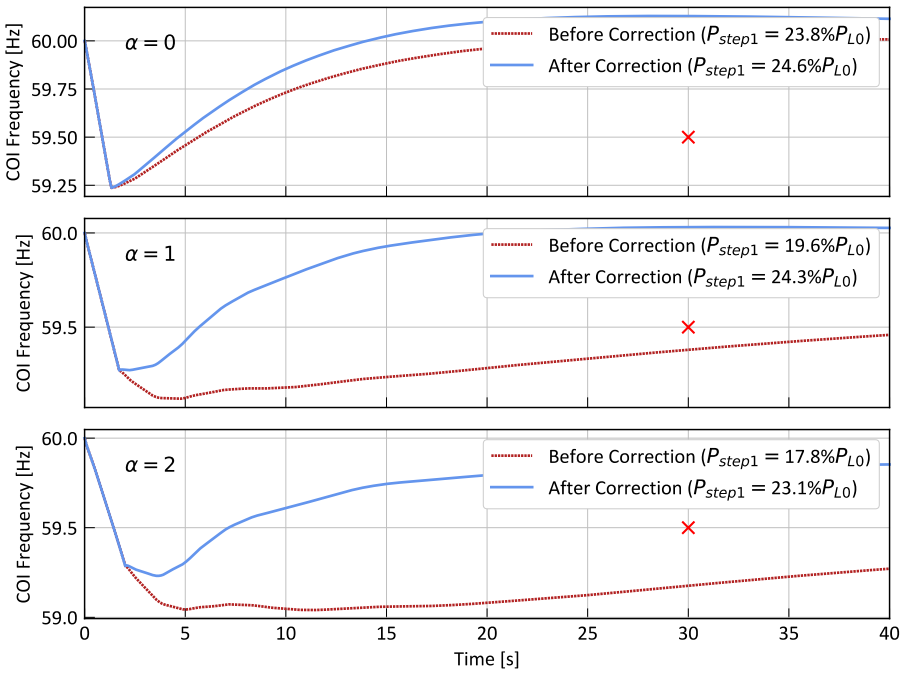

Figure 4-14: Testing Step Correction in Scenario D

From the simulation results in the above four separation scenarios, the correction step is generally effective in balancing the two trade-off factors, namely reduction in total shedding amount and compliance with the IEEE objectives. However, as observed in scenario C and D, the corrected step is not as effective as in other cases when α value is low (i.e. equals to 0). This is partially because the

estimation error is larger when α equals to 0, which may lead to an inaccurate correction. How to reduce these errors remains to be further investigated.

4.7.3 Testing Step Correction with Random Load Power Dependency Values

It should be noted that in the simulation all the loads in the system are assumed to have the same voltage dependency factor, which is mentioned as an important assumption in section 3.5. To weaken this assumption and extend the simulated validity to practice, another set of simulations where all the loads α values are randomly selected (in the range from 0 to 2 with an increment of 0.1) are also proceeded.

Results of scenario C and D with random α value are shown below. In these figures, the "average" α is calculated using the pre-fault load power as the weight factor.

$$\alpha_{average} = \frac{\sum_{i=1}^{N_L} P_{L0i}\alpha_i}{\sum_{i=1}^{N_L} P_{L0i}} \tag{4-5}$$

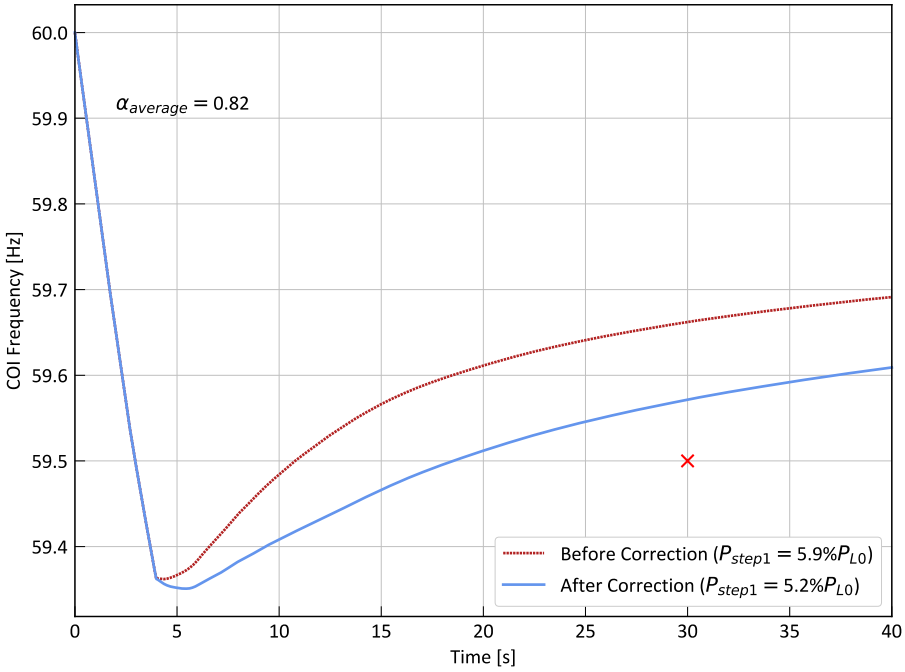

Figure 4-15: Testing Step Correction in Scenario C (Random Load Power Dependency on Voltage)

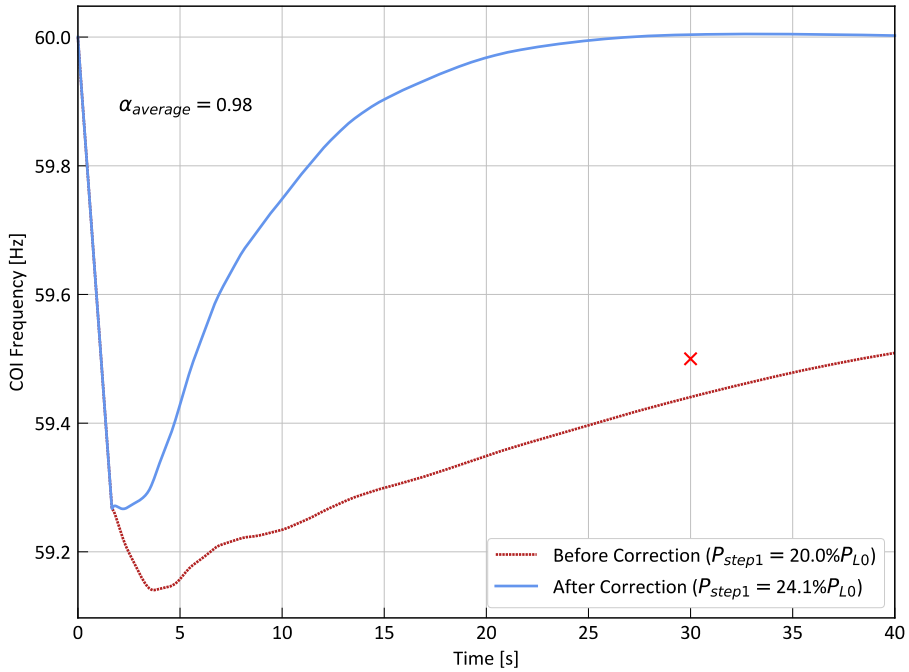

Figure 4-16: Testing Step Correction in Scenario D (Random Load Power Dependency on Voltage)

From Figure 4-15 and Figure 4-16, it is observed that the step correction method is effective on a system with random α distribution. For small disturbance (scenario C), the correction can improve frequency behavior by reducing the shedding amount, while in a more sever situation (scenario D) it slightly increases the shedding amount so as to satisfy the IEEE objectives.

4.8 Conclusion

The UFLS scheme [24] that uses ROCOF change to dynamically adapt the shedding step is modeled and implemented. Simulation results show that it can successfully arrest the frequency decline in various power system separation scenarios, and meanwhile reduce the total shedding amount to a certain degree.

It is also observed that the load shedding performance is affected mainly by two factors, i.e. the initial step size and the load power dependency on voltage. From the simulative comparison of different step distribution cases, it is found that only when the first step is equal to the estimated power deficiency can the UFLS comply with both the IEEE objectives. However, other initial step sizes can also prevent the frequency decrease below 58.5Hz and can be considered valid if the evaluation criterion is less strict.

In terms of the influence of load power dependency on voltage α, simulation results show that larger α leads to smaller total shedding amount because the load power decrease due to voltage decrease is interpreted by the UFLS relay as a temporary mitigation of the power imbalance. This phenomenon has a two-fold effect. For a power imbalance scenario that is less severe, it can reduce the total shedding amount. But for a greater disturbance, the frequency behavior may not be able to comply with the IEEE goals.

Thus, a step correction method is proposed to re-calculate the step size taking both the magnitude of disturbance (P_{def}) and load characteristics (α) into account. Results show that the corrected UFLS scheme has improved performance in different separation scenarios and load conditions.

5 Implementation of Topology-Oriented UFLS

Chapter Summary: In this chapter two topology-oriented UFLS schemes are implemented to compare their load shedding performance. The first scheme uses power flow tracing as the main factor to distribute the load shedding amount among all the loads, while the second uses the bus voltage sensitivity on reactive power to achieve the distribution of load shedding amount. Then these two schemes are simulated in various scenarios.

5.1 Introduction

Apart from the step-oriented advanced schemes, some UFLS programs proposed in the literature focus on how to allocate a pre-calculated shedding amount to the loads in the island with power deficiency. For simplicity in analysis, the proposed schemes assume to have only one shedding step, which takes place when frequency reaches the corresponding threshold (59.4Hz in the thesis case). Different allocation methods result in different distribution of shedding amount within all the loads in an attempt to decide the distance between each load and the disturbance location. From chapter 2 it is known that the distribution is based on equation (2-7) where the ith load shares a K_i proportion of the total amount.

In the thesis, the method proposed [34] and [35] are introduced and analyzed. They use power flow tracing method and voltage sensitivity method respectively to calculate the distribution factor K_i.

5.2 Power Flow Tracing Method

Power flow tracing method was originally introduced to enhance the transparency in operation of the transmission system [41]. The methodology is based on a so-called proportional sharing assumption, which, although has not been proven, can be rationalized and results in optimal operation cost allocation [42]. Through a series of matrix calculation and rearrangement, the power contribution to a load bus can be traced back to each of the member generation buses.

The principle of the scheme using power flow tracing method is to distribute the shedding amount, i.e. to calculate K_i according to the active power received by each load from the lost generators. Loads that are near the disturbance location will disconnect more percentage of pre-fault value when frequency reaches the threshold. The general process for calculating traced power is introduced below.

1. As the inflow of power equals to the outflow at any bus, the outflow of bus i can be defined as equation (5-1).

$$P_{outflow,i} = \sum_{j \in DG} \left| P_{flow,ij} \right| + \sum_{j \in DG} \left| P_{loss,ij} \right| + P_{L0i} \tag{5-1}$$

where DG is Set of buses supplied by bus i, also known as the downstream buses of i

$P_{flow,ij}$ is Active power flow from bus i to bus j

$P_{loss,ij}$ is Active power loss of line connecting bus i and bus j

2. Then a downstream distribution matrix $\boldsymbol{A}_d$ is defined with corresponding entries $[A_d]_{ij}$ as per equation (5-2). The matrix is square with dimension of $N_B \times N_B$ where N_B is the number of buses in the island.

$$[A_d]_{ij} = \begin{cases} 1, & if\ j = i \\ \dfrac{-\left| P_{flow,ij} \right|}{P_{outflow,j}}, & if\ j \in DG \\ 0, & \text{otherwise} \end{cases} \tag{5-2}$$

3. The active power contributed by generators on bus j to the load at bus i is calculated.

$$P_{Gj,Li} = \frac{P_{G0j} P_{L0i}}{P_{outflow,j}} \boldsymbol{e}_j^T \boldsymbol{A}_d^{-1} \boldsymbol{e}_i \tag{5-3}$$

where P_{G0j} is Active power supplied by the generators at bus j

$\boldsymbol{e}_i$ is Unit column vector where the gth element equals to 1 and others are zeros

4. The above the equations tracing power flow from generators to loads can be used to define the load shedding amount distribution.

$$P_{tracing,i} = \sum_{Gj \in TG} P_{Gj,Li} \tag{5-4}$$

where $P_{tracing,i}$ is Pre-fault total active power at ith load bus received from TG

TG is Set of tripped generators

5. The distribution factor is calculated using the combination of traced active power and frequency deviation.

$$K_i = \Delta f_i P_{tracing,i} \tag{5-5}$$

6. As for reactive power, it is assumed that the power factor of each load remains constant, thus

$$Q_{shed,i} = P_{shed,i} \frac{Q_{L0i}}{P_{L0i}} \tag{5-6}$$

5.3 The Voltage Sensitivity Method

The method proposed by D. Prasetijo involves bus voltage-reactive power sensitivity (VQS) as the distribution factor. Its principle is to obtain the voltage change of each bus due to the change of reactive power flow. It is calculated with the following steps.

1. Obtain the Jacobian matrix using equation (5-7).

$$\begin{bmatrix} \frac{\partial P_2}{\partial \delta_2} & \cdots & \frac{\partial P_2}{\partial \delta_N} & \frac{\partial P_2}{\partial |V_2|} & \cdots & \frac{\partial P_2}{\partial |V_N|} \\ \vdots & \boldsymbol{J}_{P\delta} & \vdots & \vdots & \boldsymbol{J}_{PV} & \vdots \\ \frac{\partial P_N}{\partial \delta_2} & \cdots & \frac{\partial P_N}{\partial \delta_N} & \frac{\partial P_N}{\partial |V_2|} & \cdots & \frac{\partial P_N}{\partial |V_N|} \\ \frac{\partial Q_2}{\partial \delta_2} & \cdots & \frac{\partial Q_2}{\partial \delta_N} & \frac{\partial Q_2}{\partial |V_2|} & \cdots & \frac{\partial Q_2}{\partial |V_N|} \\ \vdots & \boldsymbol{J}_{Q\delta} & \vdots & \vdots & \boldsymbol{J}_{QV} & \vdots \\ \frac{\partial Q_N}{\partial \delta_2} & \cdots & \frac{\partial Q_N}{\partial \delta_N} & \frac{\partial Q_N}{\partial |V_2|} & \cdots & \frac{\partial Q_N}{\partial |V_N|} \end{bmatrix} \begin{bmatrix} \Delta\delta_2 \\ \vdots \\ \Delta\delta_N \\ \Delta|V_2| \\ \vdots \\ \Delta|V_N| \end{bmatrix} = \begin{bmatrix} \Delta P_2 \\ \vdots \\ \Delta P_N \\ \Delta Q_2 \\ \vdots \\ \Delta Q_4 \end{bmatrix} \tag{5-7}$$

2. To extract the relation between reactive power and voltage magnitude, here it is assumed that $\Delta P_i = 0$. According to reference [25] and [43], a $\boldsymbol{J}_R$ matrix can be obtained.

$$\Delta \boldsymbol{Q} = \left[\boldsymbol{J}_{QV} - \boldsymbol{J}_{Q\delta}\boldsymbol{J}_{P\delta}^{-1}\boldsymbol{J}_{PV}\right]\Delta \boldsymbol{V} = \boldsymbol{J}_R \boldsymbol{V} \Rightarrow \Delta \boldsymbol{V} = \boldsymbol{J}_R^{-1}\Delta \boldsymbol{Q} \tag{5-8}$$

3. Instead of calculating $\boldsymbol{J}_R^{-1}$ directly, a decomposition method is applied. Then the above equation can be written as

$$\Delta \boldsymbol{V} = \boldsymbol{E}_R \boldsymbol{\xi}^{-1} \boldsymbol{E}_L \Delta \boldsymbol{Q} = \sum_i \frac{\boldsymbol{E}_{R,i}\boldsymbol{E}_{L.i}}{\lambda_i} \tag{5-9}$$

$$VQS_i = \frac{\partial V_i}{\partial Q_i} = \sum_i \frac{\mu_{ij}\eta_{ji}}{\lambda_j} \tag{5-10}$$

where $\boldsymbol{E}_R$ is Right eigenvector matrix of $\boldsymbol{J}_R$
$\boldsymbol{E}_L$ is Left eigenvector matrix of $\boldsymbol{J}_R$
$\boldsymbol{\xi}$ is Diagonal eigenvalue matrix of $\boldsymbol{J}_R$
$\boldsymbol{E}_{R,i}$ is ith column of $\boldsymbol{E}_{R,i}$
$\boldsymbol{E}_{L,i}$ is ith row of $\boldsymbol{E}_{L,i}$
λ_i is ith eigenvalue of $\boldsymbol{J}_R$
μ_{ij} is ith row, jth column element of $\boldsymbol{E}_R$
η_{ji} is jth row, ith column element of $\boldsymbol{E}_L$

4. The distribution factor for VQS method is calculated.

$$K_i = \frac{\Delta V_i}{VQS_i} \tag{5-11}$$

5.4 Implementation in PowerFactory

To simulate the above two UFLS schemes, the same block diagram as shown in Figure 3-9 is used. Some variations of the previous PowerFactory models are introduced to the relay and gain blocks.

First, the original "scaling factor" as the output of the relay block serves as a trigger signal in this case. When measured center of inertia frequency reaches the pre-defined threshold $f_{th,1}$, this trigger signal changes from 0 to 1.

Accordingly, the input of load gain block becomes the same trigger type. Four parameters are assigned to each corresponding load gain block ($P_{L0i}, Q_{L0i}, P_{shed}$ and K_i). P_{shed} is the total initial shedding amount in MW. When trigger signal changes from 0 to 1, the dual output of gain blocks changes from (P_{L0i}, Q_{L0i}) to $(P_{L0i} - P_{shed,i}, Q_{L0i} - Q_{shed,i})$.

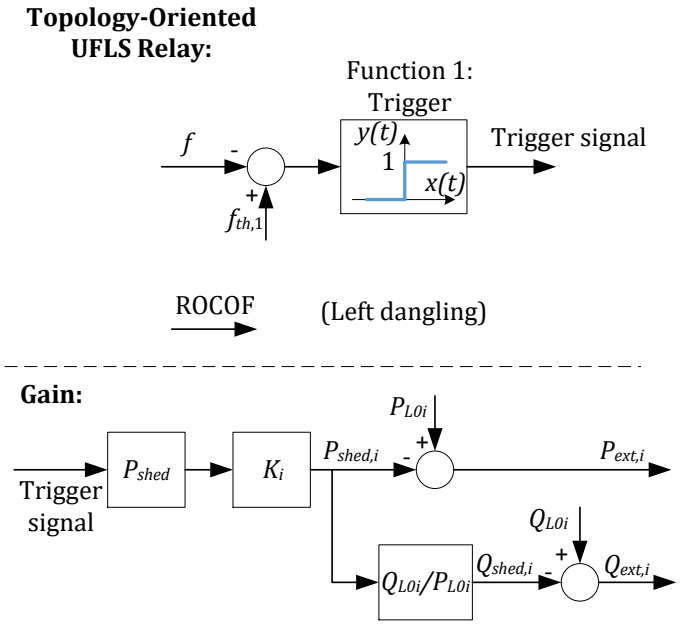

Figure 5-1: Graphical Mechanics of the Topology-Oriented UFLS Schemes

Same as in chapter 4, the frequency threshold equals to 59.4Hz and delay time is 0.3s for the topology-oriented UFLS relay.

5.5 Comparing Two Schemes in Separation Scenario A

In the simulation, the two methods mentioned above, i.e. voltage sensitivity and power flow tracing methods are compared in scenario A, which is shown in Figure 4-3. The frequency recovery is shown in Figure 5-2, while in Figure 5-3 the load shedding percentage is listed as bar graph to compare the two schemes. During the simulation, As the load shedding amount distribution is very similar when α changes, therefore only one α case is shown in Figure 5-3.

In terms of frequency, these two schemes have very similar outcome, mainly because the total shedding amounts are the same, which is the estimated value prior to the triggering of the UFLS scheme. Even though load voltage dependency factor α changes from 0 to 2 in the simulations, the overall frequency behavior remains stable and acceptable.

In terms of load shedding distribution, it can be observed that power flow tracing has a more polarized distribution of the shedding amount. Load 15 and Load 18, which are nearest to the disturbance location (Bus 16) compared to other loads, have the highest shedding amount. In comparison, the voltage sensitivity method has a flatter distribution, with every load shedding a certain percentage that ranges from 5% to 25%.

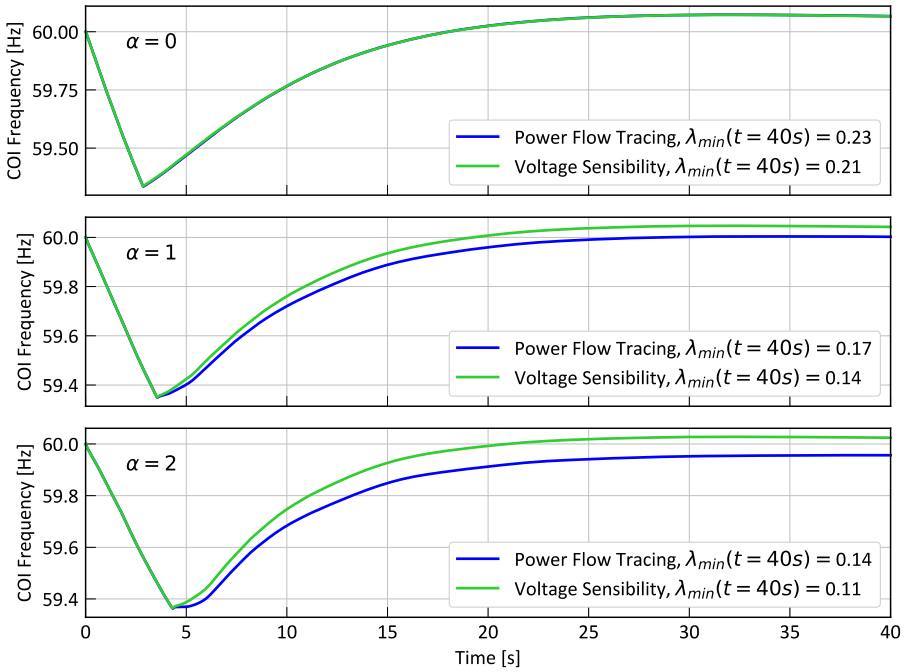

Figure 5-2: Comparing Frequency Behavior of Two Schemes in Scenario A

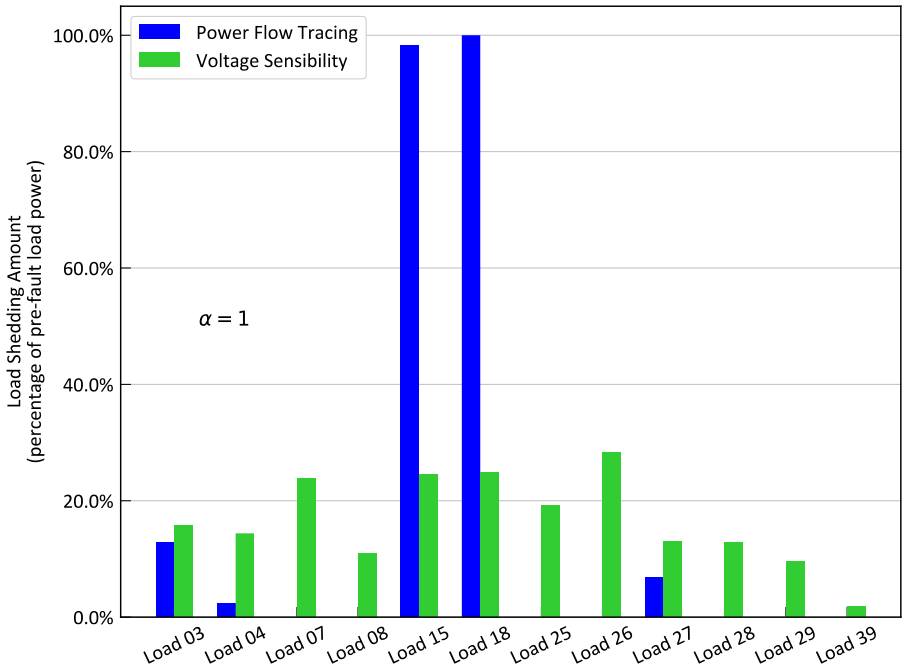

Figure 5-3: Comparing Load Shedding Amount Distribution of Two Schemes in Scenario A

As $\boldsymbol{J}_R$ matrix represent the voltage sensitivity of island buses, the minimum eigenvalue of $\boldsymbol{J}_R$ represents the smallest voltage stability among all the island buses. A positive eigenvalue means the bus voltage is stable, and negative value means it is unstable [35]. In the figure, λ_{min} is calculated at the end of the simulation time since at this stage the system frequency and voltage no longer have significant oscillation and can be regarded as a steady state. From the result, it is observed that power flow tracing method in general has a larger λ_{min} than voltage sensitivity method, meaning that it has a better voltage stability after the load shedding process.

5.6 Comparing Two Schemes in Separation Scenario B

The two schemes are also implemented in scenario B which is introduced in Figure 4-5. The power imbalance is more severe in this situation and the same conclusion can be drawn from the following results. Again, the two schemes have very similar frequency behavior, and power flow tracing has a better system voltage stability, regardless of α values.

During the implementation, another significant difference between these two methods is the computational effort that is involved in calculating the shedding amount distribution index K_i.

The calculation of voltage sensitivity costs up to several minutes in the simulation environment. As the simulation step size in PowerFactory is 0.01s, the total number of time stamps is more than 4000, considering starting time is -0.2s (slightly ahead of the separation time to avoid initial error). At each time stamp the program proceeds a decomposition for the voltage sensitivity matrix $\boldsymbol{J_R}$, whose dimension depends on the number of buses in the island. Therefore, the calculation time is significantly longer when the formed island contains more buses.

On the contrary, because power flow status in a system does not change abruptly, the pre-fault data can be regarded as readily accessible. This feature makes the power flow tracing method advantageous over the voltage sensitivity method in terms of computational effort.

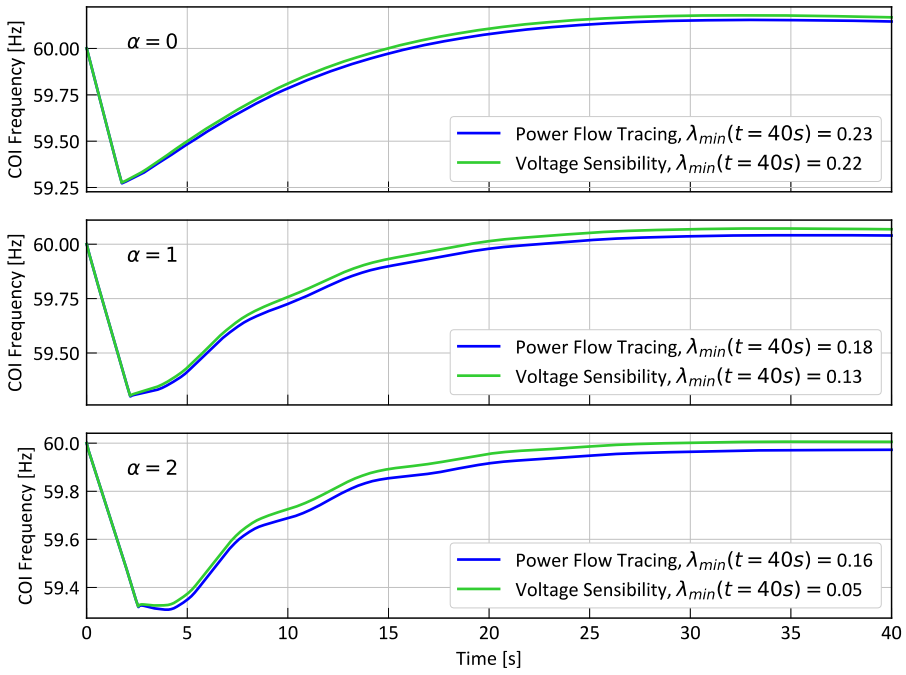

Figure 5-4: Comparing Frequency Behavior of Two Schemes in Scenario B

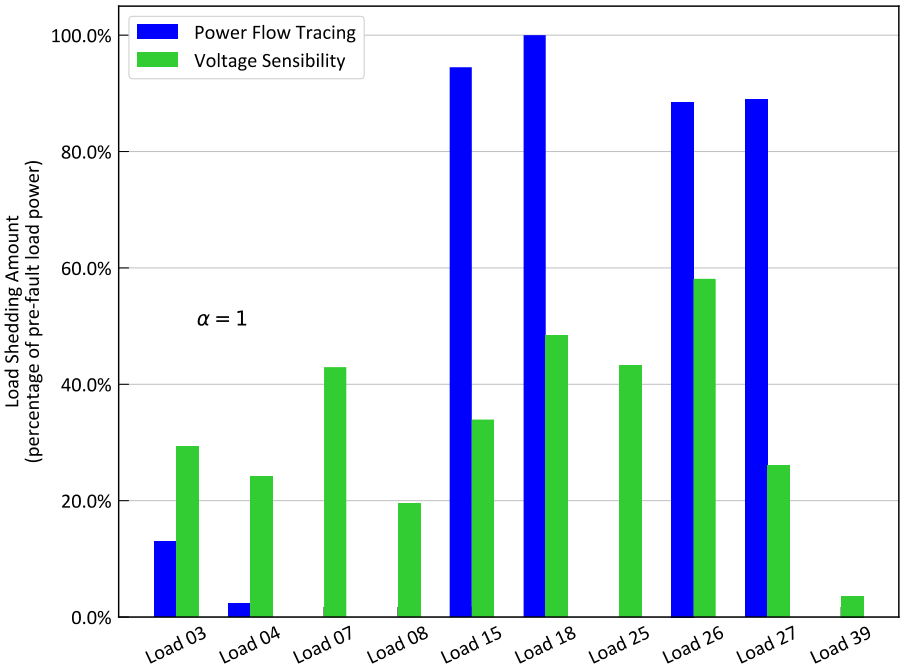

Figure 5-5: Comparing Load Shedding Percentage Distribution of Two Schemes in Scenario B

5.7 Conclusion

As introduced in the literature review, topology-oriented UFLS schemes mainly deal with the distribution algorithm for the load shedding amount among the loads. The principle is to find the distance between each load and the disturbance location from the signals of individual load such as voltage or power flow. Therefore, the set of models developed can be used for multiple such schemes if the relay definition is changed accordingly.

In the thesis, two schemes, namely power flow tracing method and voltage sensitivity method, are chosen to be implemented and compared. It is found that they are both successful in arresting the frequency decline, but power flow tracing method has better performance than voltage sensitivity method in two ways. First, power flow tracing results in a better system voltage stability, which can be seen from the eigenvalues. Second, the computational effort required in power flow tracing method is much smaller than that of voltage sensitivity method.

However, for topology-oriented UFLS schemes, there is a hidden assumption that has not been sufficiently dealt with. The fact that the disconnected power of a load cannot be larger than its pre-fault value is not mentioned in equation (2-7). If the planned shedding amount surpasses the maximum power a load can consume, the actual total shedding amount will be less than the plan and may result in a slower frequency recovery. This phenomenon can be seen from the highest bar in Figure 5-3 and Figure 5-5. The actual shedding amount of Load 18 is 100%, meaning that the initially calculated value is no less than its pre-fault active power. In addition, it can also be seen that the blue lines are slightly lower than the green lines.

Due to this hidden assumption, further improvement on topology-oriented UFLS schemes can be developed. For example, shifting the “overflowing” part of the initial shedding amount to other loads is possible to solve the issue.

6 Conclusion and Future Work

Chapter Summary: This chapter summarize the thesis content and resulting observations. Several different UFLS schemes are modeled and implemented using PowerFactory and Python. Their ability to arrest frequency decline are verified. Based on the present implementation and associated assumptions, the chapter suggests some directions that future work may follow.

6.1 Conclusion

Traditionally, under-frequency load shedding scheme consists of several pre-defined steps and frequency thresholds. But load characteristics and specific power imbalance situations are usually ignored when designing the load shedding steps, which can result in inaccurate or unsuccessful protection. In comparison, advanced UFLS schemes are based on an estimated power deficiency and an optimal load shedding amount distribution that can not only help frequency recovery, but also improve other aspects such as reducing total shedding amount, reducing computational effort, and increasing in system voltage stability.

In the thesis, a set of PowerFactory models are developed using Python for the implementation and verification of advanced UFLS schemes. The models are created in a dynamic way that can enhance the adaptability and flexibility for various advanced UFLS schemes and power imbalance scenarios.

Three representative UFLS schemes are implemented using the developed models. The first scheme, as proposed in [24], uses the real-time change of rate of change of frequency to dynamically adjust the load shedding steps and thus can reduce the total shedding amount. Simulation results show that this scheme can successfully arrest frequency decline and keep the minimum recorded frequency above the last threshold, i.e. 58.5Hz. But it may not always comply with the IEEE load shedding objectives due to the influence of both α (load power dependency on voltage) and P_{def} (magnitude of the disturbance). Thus, in section 4.7 a step correction method is proposed to improve the performance of the UFLS scheme. The correction method proves to be effective in various simulated cases.

The implementation also includes another two advanced UFLS schemes, namely power flow tracing method [35] and voltage sensitivity method [34]. These two methods prove to be effective in load shedding process and can comply with IEEE objectives under multiple circumstances. However, it is observed that power flow tracing is advantageous over voltage sensitivity in terms of both voltage stability and computational effort.

6.2 Future Work

During the implementation process, there are some issues that can be potentially improved. Future work can be focused on dealing with the following problems.

1. Improvement of power deficiency estimation.

   Figure 3-8 shows the estimation error under different conditions. In some situations, the error can be up to 9%. Since there are other factors that can affect the estimation process such as the load voltage dynamic time constant (0.1s by default in PowerFactor), they can be involved to enhance the accuracy.

2. Improvement of step correction method in section 4.7

   The step correction for the initial step in section 4.7 proves to be effective in several simulated events. However, it involves four parameters which are difficult to decide individually. In addition, when the consumed power of loads is less dependent on voltage, the correction method becomes less effective. In this matter, other approaches such as the neuro network algorithm can be used for better and more adaptive parameter configuration.

3. Improvement of the topology-oriented schemes

   It is mentioned in section 5.7 that the considered topology-oriented schemes do not sufficiently deal with the hidden assumption that the shedding amount of a load cannot be larger than its maximum power consumption. Thus, it may cause the actual shedding amount less than the planned value. Regarding this problem, further improved can be focused on the shifting of the "overflowing" part of shedding amount to other loads.

In conclusion, the thesis has developed a systematic and dynamic model for advanced UFLS schemes. By simulating and investigating several selected schemes, feasibility and implementability of both the model and the UFLS schemes are verified to have substantial improvement.

7 Reference

[1]. Andersson, G., et al. "Causes of the 2003 major grid blackouts in North America and Europe, and recommended means to improve system dynamic performance." IEEE transactions on Power Systems 20.4 (2005): 1922-1928.

[2]. Liscouski, B., and W. Elliot. "Final report on the august 14, 2003 blackout in the united states and canada: Causes and recommendations." A report to US Department of Energy 40.4 (2004).

[3]. Bo, Zeng, et al. "An analysis of previous blackouts in the world: Lessons for China′ s power industry." Renewable and Sustainable Energy Reviews 42 (2015): 1151-1163.

[4]. Hines, Paul, Jay Apt, and Sarosh Talukdar. "Large blackouts in North America: Historical trends and policy implications." Energy Policy 37.12 (2009): 5249-5259.

[5]. Kirschen, Daniel, and Goran Strbac. "Why investments do not prevent blackouts." The Electricity Journal 17.2 (2004): 29-36.

[6]. Shao, Hongbo, et al. "Determination of when to island by analysing dynamic characteristics in cascading outages." *PowerTech (POWERTECH), 2013 IEEE Grenoble*. IEEE, 2013.

[7]. Moura, Fabrício AM, et al. Steam turbines under abnormal frequency conditions in distributed generation systems. INTECH Open Access Publisher, 2012.

[8]. Lokay, H., and V. Burtnyk. "Application of underfrequency relays for automatic load shedding." *IEEE Transactions on Power Apparatus and Systems* 3.PAS-87 (1968): 776-783.

[9]. Ghaleh, A. P., M. Sanaye-Pasand, and A. Saffarian. "Power system stability enhancement using a new combinational load-shedding algorithm." *IET generation, transmission & distribution* 5.5 (2011): 551-560.

[10]. Liscouski, B., and W. Elliot. "Final report on the august 14, 2003 blackout in the united states and canada: Causes and recommendations." *A report to US Department of Energy* 40.4 (2004).

[11]. Saffarian, Alireza, and Majid Sanaye-Pasand. "Enhancement of power system stability using adaptive combinational load shedding methods." *IEEE Transactions on Power Systems* 26.3 (2011): 1010-1020.

[12]. Swanson, J. O., and J. P. Jolliffe. "Load Shedding Program in the Pacific Northwest [includes discussion]." *Transactions of the American Institute of Electrical Engineers. Part III: Power Apparatus and Systems* 73.2 (1954).

[13]. Report, AIEE Committee. "Automatic Load Shedding [includes discussion]." Transactions of the American Institute of Electrical Engineers. Part III: Power Apparatus and Systems 74.3 (1955).

[14]. Maliszewski, R. M., R. D. Dunlop, and G. L. Wilson. "Frequency actuated load shedding and restoration Part I-Philosophy." *IEEE Transactions on Power Apparatus and Systems* 4 (1971): 1452-1459.

[15]. Rowland, C. R., D. W. Smaha, and J. W. Pope. "Coordination of load conservation with turbine-generator underfrequency protection." *IEEE Transactions on Power Apparatus and Systems* 3 (1980): 1137-1150.

[16]. Concordia, Charles, Lester H. Fink, and George Poullikkas. "Load shedding on an isolated system." *IEEE Transactions on Power Systems* 10.3 (1995): 1467-1472.

[17]. Halevi, Y., and D. Kottick. "Optimization of load shedding system." *IEEE transactions on energy conversion* 8.2 (1993): 207-213.

[18]. Abusharkh, M. F., and A. A. Hiyasat. "Load shedding scheme of the Jordanian national power system." *Developments in Power Protection, 1989., Fourth International Conference on*. IET, 1989.

[19]. Grewal, Gursharan S., John W. Konowalec, and Mak Hakim. "Optimization of a load shedding scheme." *IEEE industry applications magazine* 4.4 (1998): 25-30.

[20]. Durbeck, Robert C. "Simulation of five load-shedding schedules." *IEEE Transactions on Power Apparatus and Systems* 5 (1970): 959-966.

[21]. Sauhats, A., et al. "Underfrequency load shedding in large interconnection." *PowerTech (POWERTECH), 2013 IEEE Grenoble*. IEEE, 2013.

[22]. Dalziel, Charles F., and Edward W. Steinback. "Underfrequency Protection of Power Systems for System Relief Load Shedding-System Splitting." *Transactions of the American Institute of Electrical Engineers. Part III: Power Apparatus and Systems* 78.4 (1959): 1227-1237.

[23]. Anderson, Philip M., and M. Mirheydar. "A low-order system frequency response model." *IEEE Transactions on Power Systems* 5.3 (1990): 720-729.

[24]. Rudez, Urban, and Rafael Mihalic. "Analysis of underfrequency load shedding using a frequency gradient." *IEEE transactions on power delivery* 26.2 (2011): 565-575.

[25]. Kundur, Prabha. Power system stability and control. Eds. Neal J. Balu, and Mark G. Lauby. Vol. 7. New York: McGraw-hill, 1994.

[26]. Palm, Sebastian, and Peter Schegner. "Static and transient load models taking account voltage and frequency dependence." *Power Systems Computation Conference (PSCC)*, 2016. Power Systems Computation Conference, 2016

[27]. Thompson, J. G., and B. Fox. "Adaptive load shedding for isolated power systems." IEE Proceedings-Generation, Transmission and Distribution 141.5 (1994): 491-496.

[28]. Chuvychin, V. N., et al. "An adaptive approach to load shedding and spinning reserve control during underfrequency conditions." IEEE Transactions on Power Systems 11.4 (1996): 1805-1810.

[29]. Bevrani, Hassan, Gerard Ledwich, and Jason J. Ford. "On the use of df/dt in power system emergency control." *Power Systems Conference and Exposition*, 2009. PSCE'09. IEEE/PES. IEEE, 2009.

[30]. Laghari, J. A., et al. "An intelligent under frequency load shedding scheme for islanded distribution network." *Power Engineering and Optimization Conference (PEDCO) Melaka, Malaysia*. IEEE, 2012.

[31]. Rudez, U., and R. Mihalic. "Forecast of the system frequency response for underfrequency load shedding." *PowerTech*, 2011 IEEE Trondheim. IEEE, 2011.

[32]. Zhong, Zhian. *Power systems frequency dynamic monitoring system design and applications*. Diss. Virginia Polytechnic Institute and State University, 2005.

[33]. Seethalekshmi, K., Sri Niwas Singh, and Suresh C. Srivastava. "A synchrophasor assisted frequency and voltage stability based load shedding scheme for self-healing of power system." *IEEE Transactions on Smart Grid* 2.2 (2011): 221-230.

[34]. Pasand, M. Sanaye, and H. Seyedi. "New centralized adaptive under frequency load shedding algorithms." *Power Engineering*, 2007 Large Engineering Systems Conference on. IEEE, 2007.

[35]. Tang, Junjie, et al. "Adaptive load shedding based on combined frequency and voltage stability assessment using synchrophasor measurements." *IEEE Transactions on power systems* 28.2 (2013): 2035-2047.

[36]. Pai, Anantha. *Energy function analysis for power system stability*. Springer Science & Business Media, 2012.Li, Juan. "Reconfiguration of power networks based on graph-theoretic algorithms." (2010).

[37]. "IEEE Guide for the Application of Protective Relays Used for Abnormal Frequency Load Shedding and Restoration", *IEEE Standard* C37.117-2007, 2007.

[38]. Sun, Hui, et al. "Optical Reflective Gear Tooth Sensor with Application to Rotational Speed Measurement." PCIM Europe 2015; International Exhibition and Conference for Power Electronics, Intelligent Motion, Renewable Energy and Energy Management; Proceedings of. VDE, 2015.

[39]. Liu, Cheng, et al. "Rotational Speed Measurement Based on Avago ADNS-9800 Laser Mouse Sensor." *PCIM Europe* 2016 (2016).

[40]. Li, Lin, Xiaoxin Wang, and Hongli Hu. "Speed condition monitoring of rotating machinery using electrostatic method." *2015 9th International Conference on Sensing Technology (ICST)*. IEEE, 2015.

[41]. Bialek, Janusz. "Tracing the flow of electricity." *IEE Proceedings-Generation, Transmission and Distribution* 143.4 (1996): 313-320.

[42]. Bialek, J. W., and P. A. Kattuman. "Proportional sharing assumption in tracing methodology." *IEE Proceedings-Generation, Transmission and Distribution* 151.4 (2004): 526-532.

[43]. Gao, Baofu, G. K. Morison, and Prabhashankar Kundur. "Voltage stability evaluation using modal analysis." *IEEE Transactions on Power Systems* 7.4 (1992): 1529-1542.

8 Appendix

8.1 Step-Oriented UFLS Relay Definition in PowerFactory

PowerFactory models are created by a Python program, which writes necessary parameters and equations in the corresponding window. Although the mechanics of the UFLS relay is described graphically in chapter 4, the actual definition in PowerFactory is written in DSL by Python. Figure 8-1 shows the screenshot of the parameter window of the definition of the UFLS relay that is implemented in chapter 4.

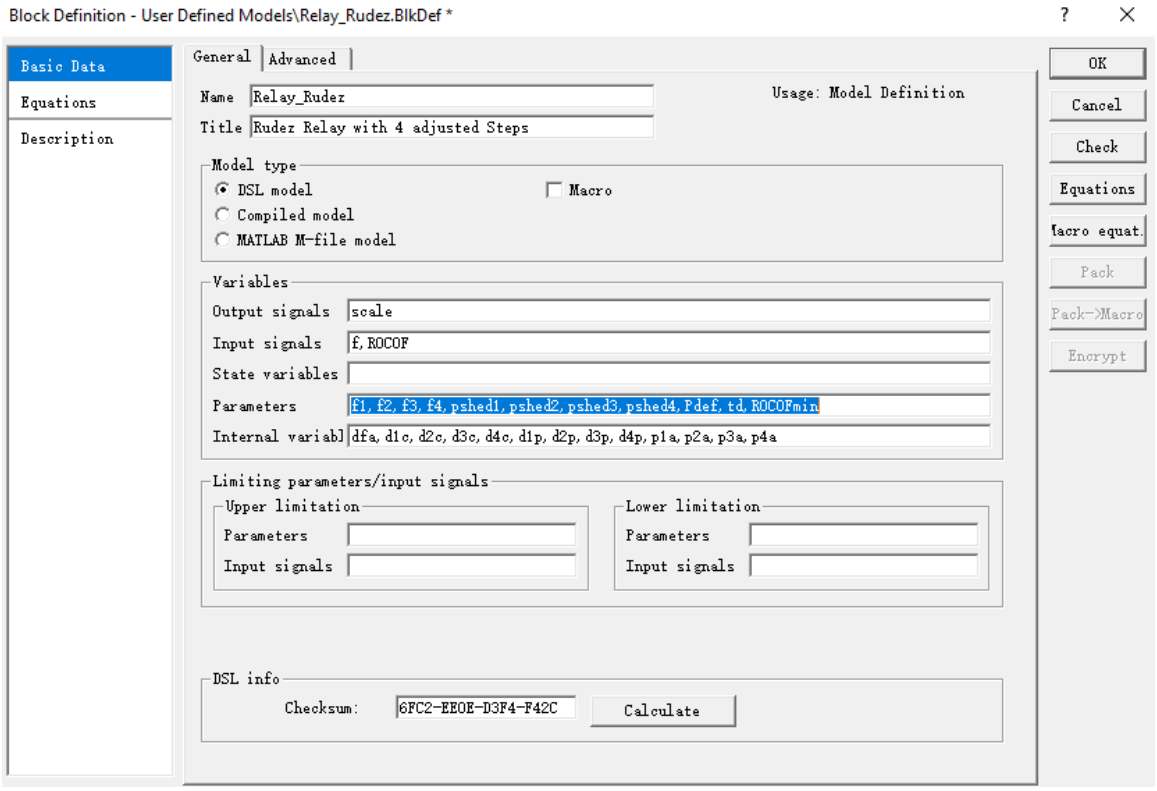

Figure 8-1: Screenshot of Step-Oriented UFLS Relay Definition Window in PowerFactory

In the "Equation" page, the mechanics of the UFLS relay, as described in chapter 4, is written in DSL as listed below.

```
! Relay definition proposed in ref [24]
dfa=select(time()>=0,ROCOF,0)
! Use dfa to avoid the initial error
! d1c,d2c,d3c d4c are changes of ROCOF [Hz/s] between steps
```

```
d1c=aflipflop(dfa-ROCOFmin,f<=f1,0)*flipflop(f<=f1,0)
d2c=aflipflop(dfa-ROCOFmin*(1-pshed1),f<=f2,0)*flipflop(f<=f2,0)
d3c=aflipflop(dfa-ROCOFmin*(1-pshed1-pshed2),f<=f3,0)*flipflop(f<=f3,0)
d4c=aflipflop(dfa-ROCOFmin*(1-pshed1-pshed2-pshed3),f<=f4,0)*flipflop(f<=f4,0)
! d1p,d2p,d3p d4p are relative change w.r.t. ROCOFmin
d1p=max(d1c/(0-ROCOFmin),0)
d2p=max(d2c/(0-ROCOFmin),0)
d3p=max(d3c/(0-ROCOFmin),0)
d4p=max(d4c/(0-ROCOFmin),0)
! Adjusted load tripping amount
p1a=max((pshed1-d1p),0)*flipflop(f<=f1,0)
p2a=max((pshed2-d2p),0)*flipflop(f<=f2,0)
p3a=max((pshed3-d3p),0)*flipflop(f<=f3,0)
p4a=max((pshed4-d4p),0)*flipflop(f<=f4,0)
scale=delay(lim(1+Pdef*(lim(p1a,0,1)+lim(p2a,0,1)+lim(p3a,0,1)+lim(p4a,0,1)),0,1),td)
inc(f)=60
inc(ROCOF)=0
inc(scale)=1
```

Notes:

1. PowerFactory standard functions are shown in blue color; comments are in green, and numbers are in red.
2. Standard function: **`select`**`(booleanexpr,x,y)`

   Returns `x` if `booleanexpr` is true, else return `y`.
3. Standard function: **`aflipflop`**`(x, boolset, boolreset)`

   Returns the old `x` value when `boolset=1` and `boolreset=0`;

   Else returns the current value of `x`.
4. Standard function: **`flipflop`**`(boolset, boolreset)`

   Changes from 0 to 1 if `boolset=1` and `boolreset=0`

   Changes from 1 to 0 if `boolset=0` and `boolreset=1`

   Remains unaltered in other situations.
5. Standard function: **`lim`**`(x,min,max)`

   Returns min if `x<min`;

   Returns max if `x>max`;

   Else returns `x`.
6. Standard function: **`inc`**`(x)`

   Initialize the signal `x`.
7. Standard function: **`delay`**`(x,Tdelay)`

   Delay function. Stores the value `x(Tnow)` and returns the value `x(Tnow-Tdelay)`. `Tdelay` must be given in seconds. In the case that it is smaller than the integration step size, the latter is used. The expression `Tdelay` must evaluate to a time-independent constant and may therefore only consist of constants and parameter variables. The expression `x(t)` may contain other functions.

8.2 Topology-Oriented UFLS Relay Definition in PowerFactory

As mentioned previously, the considered topology-oriented UFLS schemes assume to have only one shedding step for simplicity of analysis. Therefore, the model definition needs less commands. The parameters window is shown in Figure 8-2.

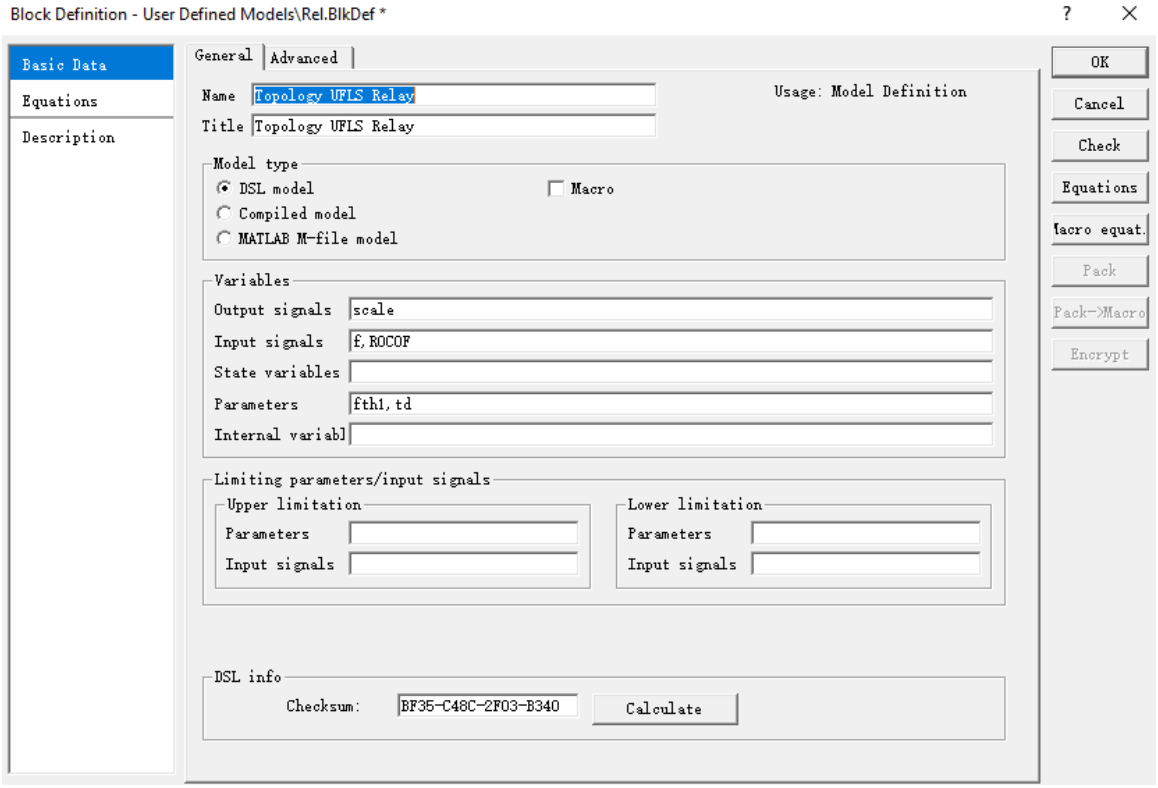

Figure 8-2: Screenshot of Topology-Oriented UFLS Relay Definition Window in PowerFactory

In the “Equation” window, the commands are written as follows.

```
scale=delay(flipflop(f<=fth1,0),td)
! Initialize signals
inc(scale)=0
inc(f)=60
inc(ROCOF)=0
```